

1 **A process-based model for ammonia emission from urine**
2 **patches, GAG (Generation of Ammonia from Grazing):**
3 **description and sensitivity analysis**

4
5 **A. Móring^{1,2,3}, M. Vieno^{1,2}, R.M. Doherty¹, J. Laubach⁴, A. Taghizadeh-Toosi⁵, M.**
6 **A. Sutton²**

7 [1]{University of Edinburgh, Crew Building, Alexander Crum Brown Road, Edinburgh, EH9
8 3FF}

9 [2]{NERC, Centre for Ecology & Hydrology, Edinburgh, Bush Estate, Midlothian, Penicuik,
10 EH26 0QB}

11 [3]{Hungarian Meteorological Service, Kitaibel P. u. 1, H-1024 Budapest, Hungary}

12 [4]{Landcare Research, P.O. Box 69040, Lincoln 7640, New Zealand}

13 [5]{Department of Agroecology, Aarhus University, Blichers Allé 20, DK-8830 Tjele,
14 Denmark}

15 Correspondence to: A. Móring (A.Moring@sms.ed.ac.uk)

16
17 **Abstract**

18 In this paper a new process-based, weather-driven model for ammonia (NH₃) emission from a
19 urine patch has been developed and its sensitivity to various factors assessed. The GAG model
20 (Generation of Ammonia from Grazing) is capable of simulating the TAN (total ammoniacal
21 nitrogen) and the water content of the soil under a urine patch and also soil pH dynamics. The
22 model tests suggest that ammonia volatilization from a urine patch can be affected by the
23 possible restart of urea hydrolysis after a rain event as well as CO₂ emission from the soil. The
24 vital role of temperature in NH₃ exchange is supported by our model results; however, the GAG
25 model provides only a modest overall temperature dependence in total NH₃ emission compared
26 with the literature. This, according to our findings, can be explained by the higher sensitivity to
27 temperature close to urine application than in the later stages and may depend on interactions
28 with other nitrogen cycling processes. In addition, we found that wind speed and relative

1 humidity are also significant influencing factors. Considering that all the input parameters can
2 be obtained for larger scales, GAG is potentially suitable for field and regional scale application,
3 serving as a tool for further investigation of the effects of climate change on ammonia emissions
4 and deposition.

5

6 **1 Introduction**

7 The consequences of strong emission of reactive nitrogen compounds (N_r), dominated by the
8 emission of ammonia (NH_3), are widely discussed: threatening air, water and soil quality, it
9 endangers also ecosystems as well as human health in many ways (Sutton et al., 2011, Galloway
10 et al., 2008, Fowler et al., 2013). Globally 70% of NH_3 released to atmosphere originates from
11 agricultural sources, such as livestock housing, manure management and fertilizer spreading on
12 fields (EDGAR, 2011). According to the latest available report of the UK government agency
13 DEFRA (Department for Environment Food and Rural Affairs), in the UK grazing accounts for
14 ca. 11% of the total NH_3 emission (Misselbrook et al., 2012). Although this proportion in the
15 total national emission is rather small, since two thirds of the grasslands are estimated to be
16 grazed (Hellsten et al., 2008), NH_3 emission from grazing affects a significant percentage of
17 the country.

18 As demonstrated by both laboratory and field experiments (Farquhar et al., 1980; Sutton et al.,
19 1995), ammonia exchange between atmosphere and surface is a bidirectional process and
20 dependent largely on meteorological factors, especially temperature. The direction of the net
21 NH_3 exchange at any time depends on the relative magnitude of the ambient air concentration
22 of NH_3 high above the surface and the concentration of NH_3 right above the surface (referred
23 to as the 'compensation point'). If the air concentration is the larger of the two, deposition
24 occurs; whilst in the opposite case, emission takes place.

25 During grazing, the dominant NH_3 source is urine, rather than dung (Petersen et al., 1998,
26 Laubach et al., 2013). In a urine patch ammonium (NH_4^+) is produced by urea hydrolysis.
27 Because of the equilibrium between NH_4^+ and NH_3 , increasing NH_4^+ concentration results in
28 an NH_3 compensation point that is usually higher than the ambient air concentration above the
29 urine patch. This generally leads to NH_3 emission from a urine patch. According to the literature
30 (e.g. Sherlock and Goh, 1985, Laubach et al., 2012 and the references therein) the period with
31 significant NH_3 emission lasts about 4-8 days after urine deposition.

1 The state-of-the-art NH_3 exchange models for vegetated surfaces (e.g. Burkhardt et al., 2009,
2 Flechard et al., 2013), called canopy compensation point models, use the analogy of electrical
3 circuits. In these, electrical current and potential difference represent NH_3 fluxes and the
4 difference between the NH_3 concentrations at the different levels of the canopy, respectively.
5 The model resistances capture the influence of meteorological factors and the canopy on NH_3
6 transfer. The first ‘canopy compensation point’ model (Sutton et al., 1995) took into account
7 the net NH_3 exchange with vegetation (a single-layer model), considering exchange with
8 stomata and leaf surfaces. Later the canopy compensation point approach was developed by
9 including NH_3 exchange also with soil surface (a two-layer model by Nemitz et al., 2001) and
10 different parts of the plant, such as siliques and foliage (a three-layer model by Nemitz et al.,
11 2000).

12 An example for estimating emissions from an excretal source that applies a simple
13 compensation point model is the GUANO model (Riddick, 2012; Sutton et al., 2013), which
14 simulates the processes leading to NH_3 emission from seabird excreta. In this model the
15 compensation point is calculated based on Henry’s law (for partitioning of NH_3) and the
16 dissociation of NH_4^+ over a hypothetical surface covered by guano. In calculating the
17 compensation point, the effect of meteorological factors (temperature, wind speed, solar
18 radiation, relative humidity and precipitation) are represented, furthermore, it accounts for the
19 total ammoniacal nitrogen ($\text{TAN} = \text{NH}_4^+ + \text{NH}_{3(\text{aq})}$) budget on the surface simulating the
20 conversion of uric acid content of guano to ammoniacal nitrogen. In addition, it also calculates
21 the water budget on the surface using the Penman equation for evaporation.

22 Several attempts have been made to simulate NH_3 emission from urine patches as well as grazed
23 fields. Laubach et al. (2012) published an NH_3 volatilization model from urine patches which was
24 run in an “inverse” mode to calculate soil resistance, applying also a simple compensation point
25 model. The equilibrium gaseous NH_3 concentration in the soil pores was considered as a
26 compensation point, and three resistances (a soil, an aerodynamic, and a quasi-laminar
27 resistance) were assumed between the soil and air concentration. Running the model in
28 predictive mode, simulating NH_3 emission, requires soil sampling and measurement of pH and
29 NH_4^+ concentration of soil water.

30 The approach for the process urea hydrolysis in the above mentioned model by Laubach et al.
31 (2012) is based on the earlier model of Sherlock and Goh (1985), which accounts for the NH_3
32 volatilization from urine patches and aqueous urea. This model for describing the transfer of

1 NH₃ between surface and atmosphere operates with a constant ‘volatilization exchange
2 coefficient’, rather than a system of dynamically changing resistances. Rachhpal and Nye
3 (1986) made an attempt to simulate NH₃ emission from applied urea. Although this model
4 employed a constant ‘transfer coefficient’ for NH₃ volatilization as well as a constant rate of
5 urea hydrolysis were applied, the study gives an alternative for modelling the chemistry of a
6 urine patch, as well as the vertical distribution of the different nitrogen compounds under the
7 urine patch.

8 The present paper reports our work to construct and test a process-based, weather-driven model
9 for NH₃ emission from a urine patch, which can be applied on both field and regional scales.
10 On field scale our approach is to apply the model for every urine patch deposited over the
11 modelling period (involving statistical consideration), whilst for regional scale we are currently
12 working to incorporate the field scale model into the EMEP4UK atmospheric chemistry
13 transport model (Vieno et al., 2010, 2014). As such, the development represents a contribution
14 toward developing a comprehensive suite of weather-dependent ammonia exchange models, as
15 a necessary basis for assessing the effects of climate change on ammonia emissions and
16 deposition (Sutton et al., 2013). As soil measurements are not widely available – especially for
17 a high resolution grid that would be required for regional scale application –, we had to account
18 for the relevant processes in the soil, such as the change of concentration of the different reduced
19 nitrogen compounds, pH and water content. On the other hand, bearing in mind our final goal
20 - a detailed investigation of weather dependency of NH₃ emission from grazing - we focused
21 predominantly on the parametrisation of the effect of meteorological variables, keeping the
22 simulation of physical and chemical soil processes as simple as possible.

23 As our future aim is to apply the model to regional scale, simplicity to enhance scalability is a key
24 aspect of the model development. For example, from a theoretical perspective, it could be attractive
25 to explicitly model the 3-dimensional dispersion of ammonia between urine patches and adjacent
26 vegetation within the canopy. However, this would be a much more complex task, which would
27 also require major simplification when developing an upscaled regional application.

28 In this paper we firstly provide the description of our model of Generation of Ammonia from
29 Grazing (GAG). Then we present the results from the test simulation based on the
30 measurements by Laubach et al. (2012). Finally, we report the results of a sensitivity analysis
31 in relation to the uncertain model parameters as well as several meteorological variables.

32

1 **2 Description of the GAG model**

2 To simulate NH_3 emission over a urine patch the GAG model calculates the TAN budget and
3 the water budget, as well as the soil pH (hydrogen ion, H^+ , budget) under the patch. For this
4 purpose, firstly, we assume that, during urination and rain events, the incoming liquid infiltrates
5 the soil to fill soil pores until the wetted soil layer reaches its field capacity. After this point we
6 neglect any further downward or upward motion (capillary rise) in the soil. On Fig. 1 this depth
7 in the soil is the bottom of the layer referred to as “urine affected layer”.

8 We also make the assumption that soil NH_3 emission occurs only from the ‘source layer’, the
9 very top layer of the wetted soil column (similarly to Riedo et al. 2002, who also assumed a
10 source layer on the top of their multilayer system), while reduced nitrogen (here the sum of
11 NH_x and urea) that infiltrates beneath this layer is assumed to be nitrified “and no longer
12 available to NH_3 emission. This assumption allows us to handle the numerous soil pores in the
13 source layer as a single big pore – referred hereafter as ‘model soil pore’ -, the liquid content
14 of which represents the soil pores filled by liquid, while its gaseous section represents the air-
15 filled soil pores in the source layer (Fig. 1). We assume that all the liquid content is at the bottom
16 of the model soil pore / source layer.

17 The input to the TAN budget is generated by hydrolysis of the urea contained within incoming
18 urine, while NH_3 emission acts as a loss from the TAN budget. Soil pH is also regulated by
19 urea hydrolysis, which is a proton (H^+) consuming process, and by NH_3 emission which is a
20 proton producing process. The water budget is increased by rain water and the liquid content of
21 urine, whilst it is decreased by soil evaporation. We assume that water evaporates from the
22 “evaporation layer” (as defined by Allen et al. (1998), see in more details in Section 2.5), and
23 the soil dries from the top, that is, during evaporation a dry front moves downwards in the soil.
24 The model was coded in R, version 3.1.2 (2014-10-31) (R Core Team, 2012) and the steps of the
25 calculation are shown in Fig. 2.

26 **2.1 Simulation of ammonia exchange flux**

27 As urine deposition by grazing animals typically happens on vegetated surfaces of grassland
28 we need to take into account the effect of vegetation on the total net NH_3 flux (F_t , calculating
29 as emission minus deposition) over a urine patch. Therefore, an ideal model should capture not
30 just the ground flux at the soil surface (F_g) (referred hereafter as ‘soil emission’), but also the

1 exchange with foliage (F_f), including NH_3 deposition to water and waxes on the leaf surface
 2 (F_w) and the NH_3 exchange with stomata (F_{sto}).

3 To achieve this, we extended the framework of the two-layer canopy compensation point model
 4 (abbreviated in this paper to 2LCCPM) of Nemitz et al. (2001) (Fig. 3). The original exchange
 5 model calculates F_g assuming a bulk soil compensation point on the soil surface. Instead of
 6 calculating this compensation point, we derive the compensation point for our model soil pore
 7 (χ_p). To capture the constraint due to soil particles on NH_3 exchange with the soil, we added a
 8 soil resistance (R_{soil}) to the original framework.

9 Based on the analogy of electrical circuit, seven equations (Eq. (1)-(7)) can be derived to
 10 determine the five unknown fluxes (F_t , F_g , F_f , F_w , F_{sto}) and the two unknown compensation
 11 points (over the vegetation, χ_c , and over the whole canopy, χ_{z0}). Parametrising the resistances -
 12 aerodynamic (R_a) and quasi-laminar resistance (R_b) over the canopy, aerodynamic resistance
 13 within the canopy (R_{ac}), quasi-laminar resistance (R_{bg}) at the ground, soil resistance, resistance
 14 to water and wax on the leaf surface (R_w) and stomatal resistance (R_{sto}) - as well as calculating
 15 the compensation point in the soil pore and in the stomata (χ_{sto}), we get a solvable linear system
 16 of equations.

$$F_t = F_g + F_f \quad (1)$$

$$F_f = F_w + F_{sto} \quad (2)$$

$$F_t = \frac{\chi_{z0} - \chi_a}{R_a} \quad (3)$$

$$F_g = \frac{\chi_p - \chi_{z0}}{R_{ac} + R_{bg} + R_{soil}} \quad (4)$$

$$F_f = \frac{\chi_c - \chi_{z0}}{R_b} \quad (5)$$

$$F_w = \frac{-\chi_c}{R_w} \quad (6)$$

$$F_{sto} = \frac{\chi_{sto} - \chi_c}{R_{sto}} \quad (7)$$

17 Assuming that the changes are close to linear within a time step (1h), and taking the air
 18 concentration of ammonia high above the canopy (χ_a) from measurements, the system of

1 equations was solved for every time step by using the solve function of R programming
2 language.

3 **2.2 Parametrisation of the resistances and stomatal compensation point (R_a ,** 4 **R_b , R_{ac} , R_{bg} , R_w , R_{sto} , χ_{sto})**

5 The detailed parametrisation of the resistances and the stomatal compensation point can be
6 found in Section S1 in the supplementary material together with all the model constants (Table
7 S1). Here we focus on the modifications and model assumptions we made for applying the
8 2LCCPM of Nemitz et al. (2001) in the GAG model.

9 Atmospheric resistances (R_a , R_b , R_{ac} , R_{bg}) are usually derived for homogenous (virtually infinite)
10 surfaces, which is in apparent contradiction with the current application for a single, finite urine
11 patch. In ongoing and future work we will apply the GAG model to field and regional scales,
12 where the meteorological measurements and the canopy specific parameters, required to
13 calculate these resistances, can be obtained for overall canopy types. To apply atmospheric
14 resistances to urine patches, we assume that all the required variables and parameters to
15 calculate them are representative for the whole experimental site including every single urine
16 patch on the field (we also compared the results from GAG with measurements from a field
17 experiment, as detailed in Section 4).

18 In the original description of the 2LCCPM, Nemitz et al. gave a parametrisation for R_a as a
19 function of u^* (friction velocity) and L (Monin-Obukhov length), which were measured in the
20 original modelling study. In the absence of measurements to obtain u^* and L , parametrisation
21 should be used (Eq. (S7) and Eq. (S8), respectively). As these two parameters depend on each
22 other, we applied iteration to calculate both. For R_b we applied the formula suggested by Nemitz
23 et al., expressed by Eq. (S12).

24 Following Nemitz et al., R_{ac} was assumed to be inversely proportional to u^* ($R_{ac} = \alpha u^{*-1}$).
25 Massad et al. (2010b) recommended values for parameter α for many surface types - including
26 grass - as well as for all of the four seasons (Table S1). Nemitz et al. applied a parametrisation
27 for R_{bg} (sm^{-1}) for oilseed rape (Eq. (S13)). As the approach for calculation of this resistance for
28 grasslands is not widely discussed in the literature, we adapted the one for oilseed rape for
29 grassland. In our model, soil emission is dependent also on R_{soil} , which is larger at least by one
30 order of magnitude than any of the atmospheric resistances. Thus, our model is not highly

1 sensitive to this approximation for R_{bg} (for detailed analysis of the model sensitivity see Section
2 5).

3 The cuticular exchange of ammonia is strongly linked to the presence of a water film on the
4 waxy leaf surface (Flechard et al., 1999). This can form even below the saturation point for
5 pure water vapour, as a result of condensation facilitated by hygroscopic particles on the plant
6 surface (Burkhardt et al., 1999). Therefore, the cuticular resistance (R_w) describes the effect of
7 this water film on NH_3 absorption. The extent to which such a thin water layer is present affects
8 the value of R_w ; however, NH_3 absorption is also dependent on the air concentration of the
9 acidic components (especially SO_2). These compounds, decreasing the pH of the water film,
10 favour NH_3 deposition (Flechard et al., 1999). The process is referred to as co-deposition of the
11 different components.

12 The modelling of this phenomenon requires the knowledge of the chemical composition of the
13 atmosphere and substantially increases model complexity. For a simpler approach, R_w ($s\ m^{-1}$,
14 Eq. (8)) can be estimated as a function of relative humidity (RH, %). For this purpose – similarly
15 also to Nemitz et al. (2001) - we used the formula from Massad et al. (2010b) (based on Sutton
16 and Fowler (1993)) with the recommended parameters in the same study ($R_{w(min)}$, minimal
17 cuticular resistance and a for grassland as reported by Horváth et al. (2005)):

$$R_w = R_{w(min)} \times \exp(a(100 - RH)) \quad (8)$$

18 In the original description of the 2LCCPM R_{sto} is parametrised based on Hicks et al. (1987).
19 Instead of this, we used a more state-of-the-art approach. As in Massad et al. (2010b), the value
20 of R_{sto} ($s\ m^{-1}$, Eq. (9)) was derived from the stomatal resistance to ozone ($R_{sto}(O_3)$, $s\ m^{-1}$), taking
21 into account the difference between the diffusivity of the two gases ($D_{O_3} / D_{NH_3} = 1 / 1.6$). On
22 the other hand, we parametrised $R_{sto}(O_3)$ (Eq. (10), where 41000 is the conversion from $mmol$
23 $O_3\ m^{-2}$ to $m\ s^{-1}$) based on LAI (values are recommended by Massad et al. (2010b) for grass if
24 not measured) applying the stomatal conductance (g_s , $mmol\ O_3\ m^{-2}$) model of Emberson et al.
25 (2000).

$$R_{sto} = R_{sto}(O_3) \times \frac{D_{O_3}}{D_{NH_3}} \quad (9)$$

$$R_{sto}(O_3) = \left(\frac{g_s \times LAI}{41000} \right)^{-1} \quad (10)$$

1 Stomatal conductance Eq. (11) is defined based on the relative conductances that express how
 2 the openness of the stomata changes in the function of the phenological state of the plant (g_{pot})
 3 (assuming that grass could grow equally over the year, $g_{pot} = 1$), light (g_{light}), temperature (g_{temp}),
 4 vapour pressure deficit (g_{VPD}) and soil water potential (g_{SWP}). The combined effect of these,
 5 through the openness of stomata, controls g_s between its maximal value (g_{max}) and its minimal
 6 value ($g_{max} \times g_{min}$):

$$g_s = g_{max} g_{pot} \max \{ g_{min}, (g_{light} g_{temp} g_{VPD} g_{SWP}) \}. \quad (11)$$

7 We followed the suggested parametrisation by Emberson et al. for g_{light} , g_{temp} and g_{VPD} (see in
 8 Section S1), but applied a different approach for g_{SWP} (Eq. (12)). As the GAG model simulates
 9 the volumetric water content of the soil (θ , $m^3 m^{-3}$; see the formulation in Section 2.5) for
 10 estimating g_{SWP} - instead of using the original parametrisation depending on the soil water
 11 potential - we adapted the approach by Simpson et al. (2012), who defined a soil moisture index
 12 (S_{MI} , Eq. (13)), based on θ , influenced also by the soil's permanent wilting point (θ_{pwp}) and field
 13 capacity (θ_{fc}).

$$g_{SWP} = \begin{cases} 1 & \text{if } S_{MI} \geq 0.5 \\ 2 \times S_{MI} & \text{if } S_{MI} < 0.5 \end{cases} \quad (12)$$

$$S_{MI} = \frac{\theta - \theta_{pwp}}{\theta_{fc} - \theta_{pwp}} \quad (13)$$

14 The stomatal compensation point, as the equilibrium gaseous NH_3 concentration in the stomata,
 15 can be derived from the temperature dependent form of Henry's law for dissolution of NH_3 (R1
 16 in Table 1) and the dissociation coefficient of NH_4^+ (R4 in Table 1). Nemitz et al. (2000) derived
 17 χ_{sto} (Eq. (14)) as a function of temperature (K) and the emission potential of the stomata (Γ_{sto}),
 18 which equals to the ratio of the NH_4^+ and H^+ concentrations ($mol dm^{-3}$) in the apoplasmic fluid
 19 in the stomatal cavity.

$$\chi_{sto} = \frac{161500}{T} \times \exp\left(\frac{-10380}{T}\right) \times \Gamma_{sto} \quad (14)$$

20 In the original 2LCCPM Γ_{sto} is an input parameter from measurements. Since the measurement
 21 of Γ_{sto} is very difficult, in models it is usually handled as a constant, parametrised or simulated
 22 by a sub-model (e.g. Massad et al., 2010a, Wu et al., 2009). As there were no Γ measurements
 23 in the experiment we used in the test simulation (nor would such measurements be available
 24 for regional scale application) and over a urine patch NH_3 exchange is dominated by soil

1 emission, we chose the parametrisation recommended by Massad et al. (2010b) for grazed
 2 fields. Eq. (15) assumes that Γ_{sto} reaches its maximum $\Gamma_{sto(max)}$ right after N application (in
 3 this case after urine deposition), and then decays exponentially with time (t_i indicates the time
 4 step, the hours spent after urine deposition, with a decay parameter τ set at 2.88×24 hours).

$$\Gamma_{sto}(t_i) = \Gamma_{sto(max)} \times \exp\left(-\frac{t_i - 1}{\tau}\right) \quad (15)$$

5 Massad et al. (2010b) proposed a parametrization, describing an empirical relationship (Eq.
 6 (16)) between the total N applied to the ecosystem (N_{app} in kg N ha⁻¹, see Eq. (17)) and the
 7 observed maximal stomatal NH₃ emission potential ($\Gamma_{sto(max)}$). To apply the formula for a
 8 urine patch, we calculated N_{app} as the total N content of the urine - the volume of urine (W_{urine} ,
 9 dm³) multiplied by its nitrogen content (c_N , gN dm⁻³) - divided by the area of the urine patch
 10 (A_{patch} , m²) (with 10 as a conversion factor between the different units).

$$\Gamma_{sto(max)} = 12.3 \times N_{app} + 20.3 \quad (16)$$

$$N_{app} = \frac{W_{urine} \times c_N}{A_{patch}} \times 10 \quad (17)$$

11 **2.3 Simulation of the soil pore (χ_p) compensation point and the soil resistance** 12 **(R_{soil})**

13 The simulation of χ_p (mol dm⁻³) is very similar in theory to that of χ_{sto} , being derived from
 14 Henry's law for NH₃ dissolution and the dissociation coefficient of NH₄⁺. In this way we get
 15 Eq. (18) (Nemitz et al., 2000), where T_{soil} is the soil temperature (K) and Γ_p is the ratio of the
 16 NH₄⁺ and H⁺ concentration in the model soil pore. In Eq. (19) Γ_p is expressed as a function of
 17 TAN concentration ($[TAN] = [NH_4^+] + [NH_{3(aq)}]$) based on the definition of dissociation
 18 constant ($K(NH_4^+)$, second column of Table 1 and its temperature dependent form in the third
 19 column).

$$\chi_p = \frac{161500}{T_{soil}} \times \exp\left(\frac{-10380}{T_{soil}}\right) \times \Gamma_p \quad (18)$$

$$\Gamma_p = \frac{[TAN]}{K(NH_4^+) + [H^+]} \quad (19)$$

1 TAN and H^+ concentration (both in mol dm^{-3}) are derived from TAN budget (B_{TAN} , g N) and
 2 H^+ budget (B_{H^+} , mol), according to their mass ratio with water budget ($B_{\text{H}_2\text{O}}$, dm^3) (Eqs. (20)-
 3 (21), where 14 is the molar mass of nitrogen). All budgets are simulated within GAG (see B_{TAN} :
 4 Section 2.4, B_{H^+} : Section 2.6, and $B_{\text{H}_2\text{O}}$: Section 2.5).

$$[TAN] = \frac{B_{TAN}}{B_{H_2O}} \cdot \frac{14}{1} \quad (20)$$

$$[H^+] = \frac{B_{H^+}}{B_{H_2O}} \quad (21)$$

5 For R_{soil} (s m^{-1}) we applied the approach by Laubach et al. (2012), as expressed in Eq. (22).
 6 This captures the effect of soil depth (Δz), that is, from how deep the soil NH_3 emission occurs
 7 on average. In the study of Laubach et al. Δz is referred as ‘source depth’, and in GAG model
 8 we consider it as the thickness of the source layer. The model experiments by Laubach et al.
 9 suggested that the distribution of Δz has a median of 0.002 m with an uncertainty factor of 2
 10 and a similar value (0.003 m) was used in the study of Riedo et al. (2002) as well. In reality the
 11 thickness of the source layer changes parallel with the moisture content of the top soil layer;
 12 however, its approximation, due to the thinness of the layer, is difficult. Therefore, at the
 13 moment our model operates with a constant Δz of 0.004 m. (In Section 5.2 we tested the model
 14 sensitivity also to Δz .)

$$R_{\text{soil}} = \frac{\Delta z}{\xi D_g} \quad (22)$$

15 According to this approach, R_{soil} is inversely proportional to soil tortuosity (ξ) and diffusivity
 16 of NH_3 (D_g). For ξ , Laubach et al. (2012) suggested the parametrisation by Millington and
 17 Quirk (1961), based on the volumetric water content as well as porosity (θ_{por}):

$$\xi = \frac{(\theta_{\text{por}} - \theta)^{10}}{\theta_{\text{por}}^2} \quad (23)$$

18 **2.4 Simulation of the TAN budget under the urine patch (B_{TAN})**

19 The amount of TAN in the model soil pore in a given time step t_i ($B_{\text{TAN}}(t_i)$, g N), depends on
 20 its value in the previous time step ($B_{\text{TAN}}(t_{i-1})$, g N) and is controlled by the amount of TAN
 21 produced during urea hydrolysis (N_{prod} , g N) and soil NH_3 emission (F_g , g N m^{-2}) calculated in

1 the previous time step (Eq. (24)). We assume that B_{TAN} before urine deposition is negligibly
 2 small (compared to that of after urine deposition). Therefore, its initial value is set to 0. The
 3 model does not allow to emit more NH_3 than TAN is available in the source layer, as it is described
 4 by Eq. 25.

$$B_{TAN}(t_i) = N_{prod}(t_i) + B_{TAN}(t_{i-1}) - F_g(t_{i-1}) \times A_{patch} \quad (24)$$

$$F_g = \begin{cases} \frac{B_{TAN}(t_{i-1})}{A_{patch}} & \text{if } (B_{TAN}(t_{i-1}) - F_g(t_{i-1}) \times A_{patch}) < 0 \\ \frac{\chi_p - \chi_{z_0}}{R_{ac} + R_{bg} + R_{soil}} & \text{otherwise} \end{cases} \quad (25)$$

5 TAN production depends on the current amount of urea nitrogen within the model soil pore
 6 (B_{urea} , g N), as well as soil temperature (T_{soil} , °C). For N_{prod} Sherlock and Goh (1985) suggested
 7 an empirical formula (Eq.(26)), with a temperature dependent parameter (A_h , Eq. (27)) and a
 8 hydrolysis constant (k_h , see Table 2).

$$N_{prod}(t_i) = B_{urea}(t_i) (1 - \exp(-A_h(t_i) \times k_h)) \quad (26)$$

$$A_h(t_i) = 0.25 \times \exp(0.0693 \times T_{soil}(t_i)) \quad (27)$$

9 Urea nitrogen content in a given time step (Eq. (28)) is determined by its value in the previous
 10 time step, the loss as conversion to TAN ($-N_{prod}$) and, in the first time step, the amount of urea
 11 nitrogen added (U_{add} , g N) with the incoming urine. In U_{add} (Eq.(29)) we take into account the
 12 dilution effect of rain and soil water on the nitrogen concentration of urine (c_n). We assume,
 13 that right after urine deposition the urea nitrogen content of urine, diluting in the total soil water
 14 ($B_{H_2O}^{Tot}$, Eq. (31)), forms a homogenous soil solution with a concentration of c_n^{Tot} (Eq. (30)).
 15 Finally, U_{add} is calculated as the product of c_n^{Tot} and the water content of the emission layer.
 16 (This will equal to $B_{H_2O}^{Tot}$ unless there is more water in the soil than can be stored in the
 17 emission layer, as indicated by $B_{H_2O}(\max)$, which is specified in the following section, see Eq.
 18 (35)).

$$B_{urea}(t_i) = B_{urea}(t_{i-1}) - N_{prod}(t_{i-1}) + U_{add}(t_i) \quad (28)$$

$$U_{add} = c_n^{Tot} \min \{ B_{H_2O}(\max), B_{H_2O}^{Tot} \} \quad (29)$$

$$c_n^{Tot} = c_n \frac{W_{urine}}{B_{H_2O}^{Tot}} \quad (30)$$

1 **2.5 Simulation of the water budget under the urine patch ($B_{H_2O}^{Tot}$, θ , B_{H_2O} ,**
 2 **$B_{H_2O(max)}$)**

3 The soil moisture content affects NH_3 emission in several ways. In the first time step when the
 4 urine is deposited, both the water content of the model soil pore and the water content of the
 5 whole urine-affected soil layer ($B_{H_2O}^{Tot}$, Eq. (31)) have an effect on emission. The thickness of
 6 the urine-affected soil layer depends on the amount of incoming liquids: urine (considering its
 7 whole volume as water) and rain (W_{rain} , dm^3). The more water is added, the more empty soil
 8 pore it can fill up and consequently, the deeper it will infiltrate.

9 We made the assumption for our model that the lowest possible volumetric water content in the
 10 soil is at permanent wilting point (θ_{pwp}) and the highest is at the field capacity (θ_{fc}), where both
 11 θ_{pwp} and θ_{fc} are expressed as fractions of total soil volume. Assuming that the initial soil water
 12 content is at θ_{pwp} , and after infiltration it rises to θ_{fc} , the volume fraction taken up by the
 13 incoming water will be $\theta_{fc} - \theta_{pwp}$. Finally, we get the total water content (incoming + soil water)
 14 in the urine-affected layer (having a volumetric water content of θ_{fc}) as:

$$B_{H_2O}^{Tot} = (W_{rain}(t_1) + W_{urine}) \frac{\theta_{fc}}{\theta_{fc} - \theta_{pwp}} \quad (31)$$

15 After urine deposition, actual volumetric water content (θ , Eq. (32)) of the source layer can be
 16 expressed as the volume of the water in the layer (B_{H_2O} , dm^3) divided by the volume of the soil
 17 column under the urine patch with a surface area of A_{patch} (m^2) and a thickness of Δz (m) (in
 18 Eq. (31), 1000 is the conversion from m^3 to dm^3).

$$\theta = \frac{B_{H_2O}}{1000 \times \Delta z \times A_{patch}} \quad (32)$$

19 The actual water content of the soil at any time step ($B_{H_2O}(t_i)$, Eq. (33)) depends on the water
 20 content in the previous time step, soil evaporation (W_{evap} , dm^3), rain events (W_{rain} , dm^3) and in
 21 the very first time step the volume of urine (e.g. if the volume of the urine is $1.5 dm^3$ then
 22 $W_{urine}(t_1)=1.5 dm^3$, otherwise 0). Both the volume of evaporation from the source layer and
 23 incoming rain to this layer are derived as the product of A_{patch} and soil evaporation (with E (dm^3
 24 m^{-2}): $W_{evap} = E \times A_{patch}$) as well as precipitation (with P ($dm^3 m^{-2}$): $W_{rain} = P \times A_{patch}$) for a m^2 ,
 25 respectively.

$$B_{H_2O}'(t_i) = \begin{cases} B_{H_2O}(\min) + W_{rain}(t_i) + W_{urine}(t_i) & \text{if } (B_{H_2O}(t_{i-1}) - W_{evap}(t_{i-1})) < B_{H_2O}(\min) \\ B_{H_2O}(t_{i-1}) - W_{evap}(t_{i-1}) + W_{rain}(t_i) + W_{urine}(t_i) & \text{otherwise} \end{cases} \quad (33)$$

1 It is not possible for more water to be evaporated from the source layer than the minimal water
 2 content (water content of the layer at θ_{pwp} : $B_{H_2O}(\min)$ (dm^3), Eq. (34)). On the other hand, (as
 3 is shown in Eq. (35)) this layer cannot store more water than the maximal water content (water
 4 content of the layer at θ_{fc} : $B_{H_2O}(\max)$ (dm^3), Eq. (36)). The excess water is assumed to infiltrate
 5 to the deeper soil layers. (In Eq. (34) and (36) 1000 is the conversion from m^3 to dm^3 .)

$$B_{H_2O}(\min) = 1000 \times \Delta z \times A_{patch} \times \theta_{pwp} \quad (34)$$

$$B_{H_2O}(t_i) = \min\{B_{H_2O}'(t_i), B_{H_2O}(\max)\} \quad (35)$$

$$B_{H_2O}(\max) = 1000 \times \Delta z \times A_{patch} \times \theta_{fc} \quad (36)$$

6 Instead of constructing a comprehensive energy balance model for GAG (driving NH_3 and
 7 water vapour flux in the same time), for simplicity's sake, to estimate the soil evaporation we
 8 adapted the dual crop method of Allen et al. (1998). The approach firstly calculates the
 9 reference evapotranspiration (ET_0 , evaporation from soil + transpiration by plants) for a
 10 reference surface (a surface covered by grass with a height of 0.12 m, a fixed surface resistance
 11 to water exchange of 70 s m^{-1} and albedo of 0.23). Then, defining a 'crop coefficient' (K_c) for
 12 the actual surface, it gives an estimation for the actual evapotranspiration ($ET = K_c \times ET_0$). In
 13 the final step K_c is split to a coefficient for transpiration and a coefficient for soil evaporation
 14 ($K_c = K_{cb} + K_e$).

15 In our model for ET_0 we incorporated a slightly modified form of the Penman-Monteith
 16 equation (Eq.(37), Walter et al., 2001) compared with that of Allen et al. (1998). In this way
 17 the model accounts for the effect of change of day and night on evapotranspiration (C_d , Eq.
 18 (38)). For the formulation of Δ (the slope of the saturation vapour pressure temperature
 19 relationship), R_n (net radiation), G (soil heat flux) and γ (psychrometric constant), see the details
 20 in Allen et al. (1998).

$$ET_0 = \frac{0.408 \times \Delta (R_n - G) + \gamma \frac{37}{T + 273.15} u (e_s - e_a)}{\Delta + \gamma (1 + C_d u)} \quad (37)$$

$$C_d = \begin{cases} 0.24 & \text{if } R_n > 0 \quad (\text{daytime}) \\ 0.96 & \text{otherwise} \quad (\text{nighttime}) \end{cases} \quad (38)$$

1 When calculating soil evaporation ($E = K_e \times ET_0$) we made the following assumptions:

- 2 - According to Allen et al. soil evaporation occurs from the wetted, uncovered soil
3 fraction (f_w). Applying the evapotranspiration model for a urine patch, the whole
4 modelled soil will be wet. In addition, we assumed that the percentage of the whole field
5 covered by vegetation (f_c) is the same over a urine patch. In this way $f_w = (1 - f_c)$ for a
6 urine patch.
- 7 - Following the recommendations of Allen et al., we assumed that there is no runoff, no
8 transpiration from the evaporation layer (including the NH_3 source layer) and no ‘deep
9 percolation’ (which occurs when θ exceeds θ_{fc} , but in our model θ_{fc} is assumed to be the
10 maximum of θ).
- 11 - In the original approach it is assumed that soil evaporation attenuates when more water
12 is evaporated from the soil evaporation layer (characterized by a thickness of Δz_E) than
13 the amount of ‘readily evaporable water’ (REW). The study of Allen et al. recommends
14 REW values for different soil types defined by their θ_{fc} and θ_{pwp} . However, for the site
15 whose measurement we used in the test simulation (see Section 4.), with a sandy loam
16 soil, these θ_{fc} and θ_{pwp} values were not in accordance with the measurements. Therefore,
17 we calculated REW as the water content of the evaporation layer halfway between θ_{fc}
18 and θ_{pwp} :

$$REW = 1000(\theta_{fc} - 0.5(\theta_{fc} - \theta_{pwp})) \times \Delta z_E \quad (39)$$

19 The model constants used in the soil evaporation estimation are listed in Table S2.

20 **2.6 Simulation of soil pH (B_{H^+})**

21 After urine deposition, soil pH is affected by two main reactions: urea hydrolysis and NH_3
22 emission. When a urea molecule is decomposed (based on R0 in Table 1) an H^+ ion is
23 consumed, producing two NH_4^+ ions and a bicarbonate ion (HCO_3^-). In the early stages of urea
24 hydrolysis, when a large amount of urea is hydrolysed, a large amount of H^+ is required,
25 resulting in a peak of soil pH (minimum of soil H^+ concentration). This triggers the dissociation
26 of the produced NH_4^+ and consequently the formation of gaseous ammonia, which also leads
27 to an emission peak shortly after urine deposition. Once the majority of urea has been

1 hydrolysed, ammonia emission may still be continuing. To balance the lost gaseous ammonia,
2 more NH_4^+ dissociates, resulting in H^+ production, which tends to compensate the H^+
3 consumption associated with urea hydrolysis.

4 According to Sherlock and Goh, (1985) after a rapid increase, soil pH usually peaks around 6-
5 48 hours after urine deposition (referred to as 'first stage' of emission). Subsequently, the pH
6 tends to drop for the reasons explained above over a period of about 2-8 days (second stage).
7 Sherlock and Goh also identified two further stages: a 1-3 week long constant phase (third
8 stage) when soil pH does not change considerably and, finally, a phase (fourth stage) with a
9 moderate decline in soil pH, regulated by the nitrification of TAN.

10 As Sherlock and Goh (1985) pointed out that the bulk of TAN is volatilized over the first and
11 second periods, and nitrification is a sufficiently slower process than NH_3 volatilization (see
12 the cited references in the study of Sherlock and Goh), in the GAG model we neglect the effect
13 of nitrification. On the other hand, we make the assumption that the solid material of soil is
14 chemically inert, and consequently, NH_3 emission from soil is only affected by the composition
15 of urine solution.

16 Whitehead et al. (1989) showed that not only urea but other urinary nitrogen components, such
17 as allantoin, creatine and creatinine, can contribute to NH_3 emission through their
18 decomposition. However, Whitehead et al. found that only allantoin can have a comparable
19 influence on NH_3 volatilization (from the solutions of these compounds with the same N
20 concentration, over 8 days 15% of the applied N was emitted from urea and 11% from the
21 allantoin); that of the other two components, creatine and creatinine, is rather small (over 8 days
22 4% and less than 1% of the applied N was emitted as NH_3 , respectively). In addition, according
23 to Dijkstra et al. (2013) the proportion of allantoin in urinary nitrogen is considerably lower
24 than that of urea, 2.2-14.2% compared to 57.8-93.5% and the proportions for creatine and
25 creatinine are even lower. Therefore, to further focus our model onto the key reactions, we
26 simulate urine chemistry considering only the water and urea available in the beginning, and
27 the products of urea breakdown afterwards.

28 As urine is a relatively concentrated solution, non-ideal ionic behaviour may have an effect on
29 the chemical equilibria. To test this in the model, we did a test run with the maximum activity
30 coefficients derived for the highest ion concentrations (0.2 mol dm^{-3}) published by Kielland
31 (1937) (the highest ionic concentration in the modelled solution was 0.14 mol dm^{-3}). With this
32 modification, the difference, in the total NH_3 emission was -4.7% and the average change in

1 pH was -0.019. Considering, that the ion concentration decreases toward the end of the
2 modelling period, and consequently, the activity coefficients converge to 1, we neglect the
3 effect of non-ideal behaviour in the solution.

4 In this way, we consider the reactions for change of soil pH listed in Table 1: urea hydrolysis
5 (R0), NH_4^+ dissociation (R1), dissociation of HCO_3^- and H_2CO_3 (carbonic acid) (R2 and R3,
6 respectively), formation of gaseous NH_3 and CO_2 (carbon dioxide) (R4 and R5, respectively).
7 However, considering that soil is a buffered system, we also incorporate a soil buffering
8 capacity ($\beta \text{ mol H}^+ (\text{pH unit})^{-1} \text{ dm}^{-3}$). Buffering capacity moderates the change of H^+ ion
9 concentration. When H^+ ions are produced in the system during urea hydrolysis and the related
10 equilibrium processes, to balance this change H^+ ions are consumed by buffers, and similarly,
11 when H^+ ions are consumed in the system, buffers releases H^+ ions. In the model this buffering
12 effect is expressed by the term of $\beta_{\text{patch}}(\text{pH}(t_i) - \text{pH}(t_{i-1}))$ in Eq. 46. This term is positive when the
13 H^+ ion concentration decreases (pH increases), and it is negative in the opposite case.

14 Whitehead and Raistrick (1993) found a strong correlation between the cation exchange
15 capacity (CEC) and NH_3 volatilization as well as a weaker correlation with organic matter, clay
16 and sand content of the soil. However, we are not aware of a specific quantitative relationship
17 between buffering capacity and CEC, or the clay content or the organic matter content.
18 Therefore, we address this issue through a sensitivity analysis on the model performance
19 (Section 5.3).

20 Regarding the effect of the potassium content of urine on buffering capacity and indirectly, NH_3
21 emission, Whitehead et al. (1989) showed that the potassium salts of urine have a rather small
22 influence on NH_3 volatilization. Based on these, we used a constant buffering capacity in the
23 model. We defined β during test simulations with GAG. We found, that the model represents
24 the measured pH well with a β of $0.021 \text{ mol H}^+ (\text{pH unit})^{-1} \text{ dm}^{-3}$. To get the buffering effect in
25 the volume of our model soil pore we calculated $\beta_{\text{patch}} = \beta \times A_{\text{patch}} \times \Delta z$. (For a sensitivity
26 analysis to β see Sect. 5.3.)

27 We defined 13 equations to calculate soil pH (Eqs. (40)-(52)), eight of which are predictive
28 equations, Eqs. (40)-(47), where B_X (mol) is the budget of the component X in the urine solution
29 and r_{R_X} (mol) is the production or consumption of the compound predicted by the given equation
30 in the reaction X (following the numbering of reactions in Table 1). Variables i_N and i_C indicate
31 the nitrogen and carbon input generated during urea hydrolysis, respectively. The nitrogen input
32 is the same as N_{prod} but in mol ($i_N = N_{\text{prod}} / 14$) and based on R0, $i_C = i_N / 2$.

1 The other five equations describe the equilibrium in every time step (Eqs. (48)-(52)). These
2 were derived by reorganizing the equations in the second column in Table 1, where, for a
3 dissolved component X: $[X] = B_x / B_{H_2O}$ and for a gaseous component $X_{(g)}$: $[X_{(g)}] = B_{X_{(g)}} / V_{air}$.
4 V_{air} is the volume of the air in the model soil pore, which can be calculated as the volume of
5 the space in the model soil pore that is not taken up by the liquid content
6 ($V_{air} = \theta_{por} A_{patch} \Delta Z \times 1000 - B_{H_2O}$, where 1000 is the conversion between m^3 and dm^3).
7 Variables B_C and B_N represent the total inorganic carbon and nitrogen budget in the urine
8 solution, respectively. Both can be derived as a sum of the different components and their input
9 (by urea breakdown) and loss (via emission as gas) (Eqs. (53) and (54)).

$$B_{H_2CO_3}(t_i) = B_{H_2CO_3}(t_{i-1}) + (-r_{R5} + r_{R3}) \quad (40)$$

$$B_{HCO_3^-}(t_i) = B_{HCO_3^-}(t_{i-1}) + (-r_{R2} - r_{R3} + i_C(t_i)) \quad (41)$$

$$B_{CO_3^{2-}}(t_i) = B_{CO_3^{2-}}(t_{i-1}) + r_{R2} \quad (42)$$

$$B_{CO_{2(g)}}(t_i) = B_{CO_{2(g)}}(t_{i-1}) + r_{R5} \quad (43)$$

$$B_{NH_4^+}(t_i) = B_{NH_4^+}(t_{i-1}) + (-r_{R1} + i_N(t_i)) \quad (44)$$

$$B_{NH_{3(aq)}}(t_i) = B_{NH_{3(aq)}}(t_{i-1}) + (r_{R1} - r_{R4}) \quad (45)$$

$$B_{NH_{3(g)}}(t_i) = B_{NH_{3(g)}}(t_{i-1}) + \left(r_{R4} - \frac{F_g(t_{i-1}) \times A_{patch}}{14} \right) \quad (46)$$

$$B_{H^+}(t_i) = B_{H^+}(t_{i-1}) - i_C(t_i) + (-r_{R3} + r_{R2} + r_{R1}) + \beta_{patch}(pH(t_i) - pH(t_{i-1})) \quad (47)$$

$$K(NH_4^+)(t_i) B_{H_2O}(t_i) B_{NH_4^+}(t_i) - B_{H^+}(t_i) B_{NH_{3(aq)}}(t_i) = 0 \quad (48)$$

$$K(CO_3^{2-})(t_i) B_{H_2O}(t_i) B_{HCO_3^-}(t_i) - B_{H^+}(t_i) B_{CO_3^{2-}}(t_i) = 0 \quad (49)$$

$$K(H_2CO_3)(t_i) B_{H_2O}(t_i) B_{H_2CO_3}(t_i) - B_{H^+}(t_i) B_{HCO_3^-}(t_i) = 0 \quad (50)$$

$$\left(H(CO_{2(g)})(t_i) \frac{B_{H_2O}(t_i)}{V_{air}(t_i)} + 1 \right) B_{H_2CO_3}(t_i) + H(CO_{2(g)})(t_i) \frac{B_{H_2O}(t_i)}{V_{air}(t_i)} B_{HCO_3^-}(t_i) + H(CO_{2(g)})(t_i) \frac{B_{H_2O}(t_i)}{V_{air}(t_i)} B_{CO_2}(t_i) =$$

$$= H(CO_{2(g)})(t_i) \frac{B_{H_2O}(t_i)}{V_{air}(t_i)} B_C(t_i) \quad (51)$$

$$\begin{aligned} & \left(H(NH_{3(g)})(t_i) \frac{B_{H_2O}(t_i)}{V_{air}(t_i)} + 1 \right) B_{NH_{3(aq)}}(t_i) + H(NH_{3(g)})(t_i) \frac{B_{H_2O}(t_i)}{V_{air}(t_i)} B_{NH_4^+}(t_i) = \\ & = H(NH_{3(g)})(t_i) \frac{B_{H_2O}(t_i)}{V_{air}(t_i)} B_N(t_i) \end{aligned} \quad (52)$$

$$B_C(t_i) = B_{H_2CO_3}(t_{i-1}) + B_{HCO_3^-}(t_{i-1}) + B_{CO_3^{2-}}(t_{i-1}) + B_{CO_2}(t_{i-1}) + i_C(t_i) \quad (53)$$

$$B_N(t_i) = B_{NH_{3(aq)}}(t_{i-1}) + B_{NH_4^+}(t_{i-1}) + B_{NH_{3(g)}}(t_{i-1}) + i_N(t_i) - \frac{F_g(t_{i-1}) \times A_{patch}}{14} \quad (54)$$

1 Although references can be found in the literature for measurements of CO₂ emission from
 2 urine patches (e.g. Wang et al., 2013, Ma et al., 2006 and Lin et al., 2009), we considered that
 3 the driving processes behind them are not well-enough described for an hourly model
 4 application. Therefore, in the case of the carbon budget (Eq. 53) we did not assume a term for
 5 CO₂ emission in the basic GAG model, but we tested the effect of CO₂ emission in Section 5.3.
 6 The dissociation coefficients (K(X)(t_i)) and Henry constants (H(X(g))(t_i)) for the given t_i time
 7 step were derived as a function of actual soil temperature (third column of Table 1).

8 For a given B_{H+}(t_i) Eqs. (40)-(46) and Eqs. (48)-(52) constitute a linear system of equations (12
 9 equations, and seven B_X(t_i) budgets and five r_{Rx} consumptions/productions as unknowns). As
 10 B_{H+}(t_i) is unknown, we are looking for a solution with a particular B_{H+}^{*} for this equation system,
 11 whose roots also satisfy Eq.(47), giving back B_{H+}^{*}. For this purpose, we used the uniroot
 12 function of programming language R (version 3.1.2 (2014-10-31)), which is able to find this
 13 B_{H+}^{*}. B_{H+}^{*} provides the H⁺ budget in the given time step and finally, pH can be calculated as
 14 pH = -log₁₀ (B_{H+}^{*} / B_{H2O})

15

16 **3 Measurement data used in the test simulation**

17 The GAG model described in the preceding sections was developed to simulate NH₃ emission
 18 from a single urine patch. However, for testing the model we chose a field experiment where
 19 the NH₃ emission flux was measured from several urine patches deposited relatively close in
 20 time. The only experiment we are aware of with these features was conducted by Laubach et

1 al. (2012), who measured the NH_3 fluxes over a field covered with a regular pattern of urine
2 patches.

3 In the experiment, 156 artificial urine patches were deposited within 45 minutes (see an
4 overview of urine patch characteristics in Table 2) over a circular plot at an experimental site,
5 in Lincoln New Zealand. In the middle of the plot NH_3 concentration was measured at five
6 heights with Leuning samplers (Leuning et al., 1985) from which the fluxes were derived by
7 different methods. For this study we used the fluxes calculated by Laubach et al. according to
8 the mass balance (MB) method.

9 Soil samples were taken from 24 patches on the edge of the plot to measure soil pH, volumetric
10 water content and mineral N content. Soil temperature was measured at two heights, and
11 meteorological measurements were also carried out (from which we used wind speed,
12 temperature, photosynthetically active radiation (PAR), sensible heat flux and atmospheric
13 pressure data). For more details on measurements and flux calculation, see Laubach et al.
14 (2012).

15 In addition to the available measurements, we also needed meteorological data that were not
16 measured in the experiment: global radiation (R_{glob}) and RH. We obtained these data from the
17 National Climate Database for New Zealand (NIWA, 2015).

18 We compared our model results with measurements of F_t , soil pH and θ for the measurement
19 period between 24/02/2010 11:30 AM and 01/03/2010 1:30 AM. In the case of F_t , the length of
20 the collecting period of each measurement varied mostly between 1-1.5 hour for daytime
21 measurements, and 7-7.5 hours for the night-time measurements. As the time step of our model
22 is 1 hour and emission fluxes were not expected to change considerably over the night, we
23 assumed that the measured average NH_3 flux over the collecting period is representative for the
24 midpoint of the period, and we compared these to our model values in the time step closest to
25 the midpoint of the corresponding measurements.

26 In addition, assuming that the change of the soil's mineral reduced nitrogen content ($\text{NH}_x\text{-N}$) is
27 parallel with the B_{TAN} in the model soil pore, we also compared these two parameters. All of
28 the input data, as well as the measurement data we used to compare our model results, together
29 with their modification for our hourly model run, are listed in Table 3.

30 To compare the measured and modelled F_t for a single urine patch, we assumed that the great
31 majority of NH_3 in the experiment of Laubach et al. (2012) was emitted from the urine patches.

1 Therefore, we multiplied the observed fluxes by the effective source area (804.9 m² as
2 calculated by Laubach et al. (2012)), then divided it by the total area of the deposited 156
3 patches (Eq. (55), F_t^{single} stands for the converted measured flux).

$$F_t^{\text{single}} = F_t \times 804.9 / (156 \times A_{\text{patch}}) \quad (55)$$

4 To compare θ with the observations, we had to consider that the θ measurements were taken by
5 using a sharp-edged metal ring that was pushed to about 5mm to the soil. As the model simulates
6 the water content of a 4 mm thick layer, the same water loss via evaporation would not result
7 in the same volumetric water content as was measured in the 5 mm depth sample. Since none
8 of the other soil modules have effect on the water budget, we ran the model also with a Δz of 5
9 mm to get results that are comparable with the measurements.

10

11 **4 Test simulation**

12 The results of the test simulation are summarized in Fig. 4 and Table 4. GAG captures the
13 emission relatively well. Considering, that compared to the complexity of the phenomena, we
14 use a simple model, the Person's correlation coefficient (hereafter referred to as "correlation")
15 for NH₃ flux, can be considered as relatively high ($r=0.54$, $p=0.01$). The model slightly
16 overestimates the fluxes before the rain event on the second day and it rather underestimates the
17 measured values after it. The total emissions over the whole period from a single patch
18 (modelled: 1.78 g N, measured: 3.88 g N) was underestimated. However, the model is still
19 capable of reproducing the daily pattern of emissions with the mid-day peaks (except on the
20 second day).

21 Soil pH is well simulated before the rain event, but similarly to the emission fluxes, it is
22 underestimated afterwards. Overall there was a high and significant correlation ($r=0.75$),
23 between the model and the measurements. The sudden pH drop at the beginning of the rain
24 event is thought to be caused by the lack of handling of CO₂ emission in the basic version of
25 the model (see Section 5.3 for further examination of this effect).

26 Despite the large error bars on the measured mineral reduced soil N, its tendency is fairly similar
27 to that of the TAN budget simulated by GAG. This is supported also by the significant
28 correlation ($r=0.63$) between the two variables. The model performance in terms of volumetric
29 water content is very good with a slight underestimation from the fourth day after urine

1 application. The statistical analysis showed a high correlation of 0.92 at a 0.001 significance
2 level.

3 Analysing the NH_3 emission, pH and TAN budget together, it can be concluded that the rain
4 event affected all three variables considerably. As it can be seen in the measured $\text{NH}_x\text{-N}$ and
5 pH dataset (Fig. 4.), their values right after the rain event peaked close to the level (or even
6 higher) of the first peaks, which were generated by urea hydrolysis. This suggests that urea
7 breakdown might restart after the rain event, explaining the difference between the modelled
8 and measured values.

9 The GAG model used here does not account for any retention of urine by vegetation; however,
10 it is possible that this occurs in reality. For example, Doak (1952) found that the urine held on
11 the leaf surfaces was 36% of fresh herbage weight. In addition, the model assumptions do not
12 allow the model soil pore to dry out (the minimum water content is at the permanent wilting
13 point). In reality, however, the moisture content of urine retained on the leaf surfaces can
14 evaporate easily and also some soil pores can completely dry out leaving behind the urine
15 components undissolved. In such dry conditions, in lack of water urea hydrolysis stops. Then,
16 after a rainfall, urea gets dissolved (as well as from the leaf surface it is washed into the soil)
17 and hydrolysis can begin again, leading to a high peak in pH, TAN budget and consequently,
18 NH_3 emission (see the further model results presented in Section S4).

19

20 **5 Sensitivity analysis for non-meteorological parameters**

21 In the following subsections we investigated module by module (2LCCPM, TAN budget, soil
22 pH and water budget), how the model responds if we change the most critical model features.
23 In the case of the model constants, we tested how the modelled total emitted NH_3 (1.78 g N
24 from a urine patch) changes over the modelling period by increasing and decreasing the given
25 assumed model constant by 10 and 20%. An overview of the results can be seen in Table 5.
26 Comments on this table are provided in the following subsections.

27 **5.1 Sensitivity to atmospheric resistances**

28 As the net NH_3 flux is dominated by the soil emission flux (shown in Fig. S1) we investigated
29 here only the influence of the atmospheric resistances that affect the soil emission: R_{soil} , R_{bg} ,

1 R_{ac} and R_a . In Fig. 5, on the logarithmic scale it can be clearly seen that R_{ac} is the only
2 atmospheric resistance that reaches the magnitude of the estimated R_{soil} .

3 For the simulation the main driver in temporal variation in R_{soil} is the actual volumetric water
4 content (see Fig. 4). In the case of R_a , R_b , and R_{bg} there is at least one order of magnitude
5 difference compared to the soil resistance, illustrating how the model performance is much less
6 sensitive to the exact values of R_a , R_{ac} , and R_{bg} . The close temporal correlation of all these
7 atmospheric resistances illustrates how they are all controlled by variations in wind speed and
8 stability for a single canopy type. All the atmospheric resistances are the closest to the soil
9 resistance when weak wind (large atmospheric resistances) is coupled to dry soil conditions
10 (small soil resistance).

11 Among R_{bg} , R_{ac} and R_a , the parametrisation of R_{bg} is the most uncertain. As Table 5 shows, the
12 model is hardly sensitive to the value of z_l . In addition, u_{*g} , as formulated by Nemitz et al.
13 (2001) (Eq. (S15)), can also change in wide ranges without significantly affecting soil emission:
14 R_{bg} could overcome the effect of R_{soil} on NH_3 emission only with a 10 times higher value of
15 u_{*g} .

16 **5.2 Sensitivity to the estimation of the TAN budget**

17 The two uncertain factors in the estimation of the TAN budget are the thickness of the source
18 layer (Δz) and the area of the patch (A_{patch}). Originally the model was run with a Δz of 4 mm;
19 however, the sensitivity analysis showed (Table 5) that the change in total emission is
20 approximately half of the change in Δz . Therefore, this source of error must be considered when
21 model results are evaluated.

22 We also tested the model with Δz values between the ranges reported by Laubach et al. (2012)
23 (Fig. 6), and we found that the smaller the value of Δz , the higher is the emission peak after
24 urine application and smaller are the emission peaks in the following days. Firstly, this is caused
25 by a smaller value of R_{soil} , due to the thinner source layer. Secondly, since the thinner layer can
26 store less TAN in total, the source layer runs out of TAN more quickly leading to lower peaks
27 in the later part of the modelling period.

28 In addition, we carried out a simulation with the maximum value of Δz , the penetration depth
29 of incoming urine. Considering that the water content of a y dm thick soil layer can be expressed
30 as $A_{patch} \times y \times (\theta_{fc} - \theta_{pwp})$, the urine deposited in a single patch (W_{urine}) in this experiment will
31 fill up a $y = 0.2$ dm = 20 mm thick soil layer. In this case, R_{soil} is at least 5 times higher than in

1 the original run (or even bigger as there is more water in the source layer consequently, the
2 layer dries out more slowly), that prevents NH_3 from escaping from the soil shortly after urine
3 deposition. However, from the second day due to the higher available TAN budget, the fluxes
4 are closer to the measurements.

5 In contrast to Δz , the model does not appear to be very sensitive to A_{patch} , with even a +20%
6 change causing less than 2% change in total emission (Table 5). Laubach et al. (2012) estimated
7 that the patches gradually grew by lateral diffusion, so that the area of the patches had doubled
8 over the modelling period at the measurement site. Therefore, we conducted a simulation with
9 GAG with a gradually growing patch, whose area doubles by the end of the period. In Fig. 7
10 we show the measured emission fluxes in relation to constant and gradually increasing values
11 of A_{patch} , with the model results expressed for the whole area (converted based on the
12 reorganized form of Eq. 55).

13 The largest difference with the growing patches, compared with the original run, occurred over
14 the first two days. Then, the emission rates became smaller for the growing patches than with
15 the constant patch area. The difference is a consequence of the combined effect of the growing
16 source area ($156 \times A_{\text{patch}}(t_i)$) and the changing emission flux from a single patch.

17 In our model if a urine patch grows, it means physically that the initial liquid content is diffusing
18 in the soil horizontally, leading to gradually declining volumetric water content. In addition,
19 the evaporating area grows simultaneously, further intensifying the decrease of water content.
20 Thus, R_{soil} will be smaller, allowing stronger NH_3 emissions in the first two days. This leads to
21 lower TAN budget in the second half of the period, resulting in slightly smaller emissions than
22 in the original run.

23 Finally, it has to be pointed out that we neglect an effect where the presence of hippuric acid in
24 urine may increase urea hydrolysis and consequently, NH_3 emission (Whitehead et al., 1989).
25 Whitehead et al. found that ignoring this triggering effect can lead to up to -10% difference in
26 the cumulative NH_3 volatilization (expressed as the proportion of the total nitrogen content of
27 urine) compared to real urine containing the same amount of urinary N.

28 In the measurement campaign (Laubach et al. 2012) an artificial urine solution was spread on
29 the experimental plot that was enriched with additional urea, so we compared a urea based
30 model with a concentrated urea solution. Therefore, the difference in modelled and measured
31 NH_3 fluxes, originating from this simplification, is possibly negligible, though it could be
32 relevant if the model is applied in real grazing situation. However, Whitehead et al (1989)

1 reported comparable differences in NH₃ emissions when they compared urea+hippuric acid
2 solutions with different total N contents as well as different hippuric acid ratios.

3 The N content of urine ranges widely, not just amongst different animals, but also for different
4 urination events by the same animal (Betteridge et al., 1986 and Hoogendoorn et al., 2010).
5 This means that assuming an average N concentration of 8 g, according to Whitehead et al.
6 (1989) can result in a 10% overestimation in the cumulative volatilization of ammonia if the
7 real nitrogen concentration was as low as 2 g/l. Similarly, in the case of the different ratios of
8 hippuric acid and urea: if we assume that the hippuric acid N is an average of 0.8% of the urea
9 N (based on the data published by Dijkstra et al. (2013) this proportion varies between 1.4 -
10 0.36%), according to Whitehead et al. (1989), the overestimation of the cumulative ammonia
11 emission can be 10% if the proportion of hippuric acid was minimal in reality.

12 As the effect of hippuric acid on urea hydrolysis is not widely investigated in the literature, at
13 the moment the current approach is the best we can achieve to simulate the decomposition
14 chemistry in urine. Although the field scale model would most likely underestimate ammonia
15 emission due to the exclusion of the effect influence of hippuric acid, this underestimation may
16 be partly balanced by the sources of overestimation in the model. Nonetheless, this uncertainty
17 should be addressed when the model is applied on field scale.

18 **5.3 Uncertainties in the estimation of soil pH**

19 The main uncertainty in the model pH calculation is the applied buffering capacity (β).
20 Apparently, the model is not highly sensitive to the tested changes of β ; however, using the
21 same β for every soil type could lead to errors in NH₃ emission estimation. Therefore, we tested
22 the model with two contrasting assumptions about buffering capacity: a) when the system is
23 totally buffered (pH is constant) and b) when there is not any buffering effect ($\beta = 0$). For the
24 constant pH scenario, we chose the soil pH measured before the deposition of the urine patches
25 (pH=6.65).

26 The results show (Fig. 8) that with a constant soil pH, GAG fails to capture the first, dominant
27 peak in emission. This suggests that dynamic modelling of pH is necessary for a proper
28 estimation of NH₃ emission. By contrast, with $\beta = 0$ the model overestimates the first emission
29 peak, while there is little difference in NH₃ fluxes in the rest of the period. Thus, with $\beta = 0$ the
30 model is still capable of reproducing the daily cycle of NH₃ emission.

1 Another feature of the model which affects the pH as well as the emission flux calculation is
2 the handling of CO₂ emission following urine deposition (as discussed in Section 2.6). A sudden
3 drop can be seen in the simulated pH at the beginning of the rain event (Fig. 4b), which tends
4 to disappear if there is no rainfall over the modelling period (Fig. 9a, blue line).

5 At the beginning of the rainfall the volume of the gaseous part of the model soil pore suddenly
6 shrinks as the liquid part grows with the incoming water. As a result (given that the base model
7 does not allow CO₂ emission), gaseous CO₂ accumulates in the soil pore and is forced to
8 dissolve into the liquid phase. This intensifies the formation of carbonic acid and its subsequent
9 dissociation, leading to significant drop in pH.

10 In the experiment by Wang et al. (2013) CO₂ emission over urine patches peaked within 8 hours
11 after urine application, while both Ma et al. (2006) and Lin et al. (2009) found that the first peak
12 of CO₂ emission occurred on the first day. In addition, Lin et al. (2009) reported a high
13 correlation ($r=0.63$) between CO₂ emission and soil temperature, suggesting a strong
14 temperature dependency (similarly, we found a correlation of 0.58 for NH₃, see Table 6).

15 Based on the above similarities between the temporal development of NH₃ and CO₂ emission,
16 to test the effect of CO₂ emission on the GAG simulations, we assumed that the amount of
17 emitted CO₂ is half of the emitted NH₃ in moles (similarly to urea hydrolysis where from one
18 urea molecule two NH₄⁺ and one HCO₃⁻ ions are produced). Even if this is a simplification for
19 CO₂ emission, the results show the potential of future more comprehensive incorporation of the
20 process into the model. By accounting for CO₂ emission the modelled pH values were found to
21 be closer to the measured ones, while the sudden drop at the start of the rain event also largely
22 disappeared (Fig. 9). As a consequence of these changes, the NH₃ emission fluxes were larger
23 before the second day and - due to the larger loss in TAN budget - were smaller in the latter
24 part of the experiment.

25 The apparently contradictory results with the assumed CO₂ emission above - better agreement
26 in pH and poorer agreement in the NH₃ fluxes - suggest that the TAN in the model soil pore is
27 depleted too early, leading to a significant underestimation of the emission fluxes in the second
28 part of the modelling period. Two scenarios can be envisaged that could cause this effect:
29 scenario 1) the simulated rate of urea hydrolysis is higher than it is in reality, or scenario 2) at
30 the experimental site fresh urea that had been intercepted by leaves and dried onto leaf surfaces,
31 was washed to the soil during the rain event, thereby maintaining NH₃ emission afterwards.

1 As we discussed in Section 4, the measurement data also suggest the feasibility of scenario 2.
2 Therefore, we tested the model – assuming that 10% of the applied urine was intercepted on the
3 leaf surface - with 1.5 g of urea washed in during the rain event (see Section S4 in the
4 supplementary material). With this assumption the modelled values were in better agreement
5 with observations not only in the case of NH_3 exchange flux (Fig. 10d) but also the TAN budget
6 and soil pH (see both at Fig. S2). These results clearly support the idea of the possible restart
7 of breakdown of the fresh urea penetrating to the soil dissolved in rain water.

8 **5.4 Uncertainties in the estimation of the water budget**

9 The GAG model is found to be sensitive to model constants related to the water budget,
10 especially field capacity, θ_{fc} (Table 5). The high sensitivity to a low value of θ_{fc} appears to be
11 because this limits the amount of urine which remains available for hydrolysis and NH_3
12 emission from the source layer. In addition, we also found large differences in total ammonia
13 emission when we modified the permanent wilting point. On regional scale it is not likely to
14 have a database of measured θ_{fc} and θ_{pwp} values over a dense grid. It is more feasible that a soil
15 texture map can be used for this purpose with recommended values of θ_{fc} and θ_{pwp} values for
16 different soil types. Both θ_{fc} and θ_{pwp} can have an uncertainty of $\pm 20\%$ (e.g. in Allen et al.
17 (1998) for sandy loam $\theta_{fc}=0.18-0.28$), similarly to the extent of modification in the current
18 sensitivity test. Therefore, at regional application, this uncertainty has to be considered when
19 interpreting the model results.

20 In addition, a limitation of the calculation of the water budget is that GAG does not account for the
21 water movement in the soil, including the effect of capillary force, diffusion of water in the soil as
22 well as the concentration of TAN and urea within the moving liquid. However, the simulation of
23 these processes is very complex. Shorten and Pleasants (2007) published a system of partial
24 differential equations describing these processes, which could be a basis for further development of
25 GAG.

26

27 **6 Sensitivity to meteorological factors**

28 For quantitative comparison, we show a variety of meteorological factors and the hourly NH_3
29 emission fluxes in Fig. 10. The NH_3 emission flux peaks almost every day shortly after midday,
30 when soil temperature reaches its maximum. The only exception is the second day after urine

1 application when the curve of emission flux stayed flat in the simulation, which was linked to
2 the rain event as discussed in the previous sections.

3 The close relationship between the soil as well as the air temperature and NH₃ emission fluxes
4 can be also seen in the calculated high correlations ($r=0.58$ and $r=0.60$, respectively). Compared
5 with the other meteorological factors (Table 6) the relationship with these two seems to be the
6 strongest. Relative humidity apparently has a slightly weaker, but still considerable role in the
7 simulated NH₃ volatilization ($r=-0.49$). Based on the correlation values, there was a weaker
8 relationship with wind speed ($r=0.40$), which may be related to the fact that simulated R_{soil}
9 provided a much larger constraint on NH₃ soil emission than the atmospheric resistances (Fig.
10 5). Global radiation as well as atmospheric pressure indicated a weaker influence (lower than
11 $r=0.40$ in absolute value) on the simulated NH₃ emission.

12 We also carried out a sensitivity analysis to the different meteorological parameters. To test the
13 sensitivity to a given parameter, we modified it, while keeping all the other parameters the
14 same, we ran a simulation with GAG. At the end of every simulation we calculated the total
15 ammonia emission over the period, and expressed it as the percentage difference compared to
16 the total emission in the original run. To get comparable results, we modified the original
17 datasets in every case by $\pm \Delta x$, calculated as 10% of the difference between the measured
18 minimum and maximum value of the given parameter over the modelling period.

19 Table 6 shows that NH₃ emission is the most sensitive to relative humidity (the differences in
20 total emission were +9.1% and -8.6%) and wind speed (the differences were -5.5% and 4.7%).
21 In addition, a relatively high difference (+4.1%) was observed in the case of global radiation
22 when its values were raised by Δx .

23 In spite of the high correlations, when soil and air temperature were modified separately, we
24 got relatively small anomalies in the total emissions (less than 3% in absolute value for both
25 soil and air temperature). However, when air and soil temperature were adjusted together
26 (assuming that the change of these two temperature parameters is parallel), the differences were
27 larger (see Table 6). Only low sensitivity was detected in the case of atmospheric pressure and
28 hourly precipitation.

29 The results for wind speed and the different temperature parameters can be easily explained.
30 Wind plays a governing role in turbulent mixing of the quasi-laminar and turbulent layer;
31 consequently, it has a considerable effects on the vertical atmospheric transfer of ammonia.

1 Regarding temperature, urea hydrolysis as well as the compensation point both in the stomata
2 and the soil pores follow an exponential function of temperature.

3 Sutton et al. (2013) used a metric, Q_{10} , to express the relative increase in NH_3 emission over a
4 range of 10°C . We derived Q_{10} by running the model with 10°C higher air and soil temperature.
5 The resulted value of 1.26 compared to that reported by Sutton et al. for grazing (4.7 for sheep
6 sites) suggest a rather modest temperature sensitivity. The model showed similarly modest
7 sensitivity when we tested it with three and five times higher N concentration in urine (allowing
8 more TAN in the later stages of the modelling period) (Table 7). Based on this results it can be
9 concluded that the lower Q_{10} values are not a consequence of the limited TAN available in the
10 later stages of the modelling period.

11 A possible explanation for the difference between the reported and the simulated temperature
12 sensitivity can be the temporal development of Q_{10} over time (Fig. 11). We calculated the Q_{10}
13 values for every time step as the ratio of the cumulative emissions from the higher temperature
14 model version and the original one, and we found that NH_3 emission is more sensitive to
15 temperature in the first six hours than in the later stages. Considering, that over a grazed field
16 urine patches are deposited in every time step, creating a peak in the individual patch emissions,
17 the total emission for the whole field will be presumably more sensitive to temperature than
18 that for a single urine patch.

19 RH has a dual effect on NH_3 emission. Firstly, it plays a vital role in the water budget and
20 secondly, it also influences the deposition of ammonia to the leaf surface. We tested the
21 sensitivity in a model scenario where relative humidity was modified only in evaporation, and
22 we observed only a +3.2% difference for $-\Delta x$ and -2.8% for $+\Delta x$ change. This clearly suggests
23 that the effect of RH on NH_3 emission in GAG is stronger through deposition to leaf surfaces
24 than through soil evaporation.

25 The physical explanation for the opposite change in RH and the total emission is that at higher
26 values of relative humidity the formation of a water film on the leaf surface is more likely. As
27 a result, deposition is more effective (see the different fluxes in Fig. S1), which will generate a
28 loss in the net emission flux over the whole system (including the exchange with soil and
29 stomata as well as the deposition to cuticle).

30 Although precipitation was shown to suppress modelled emission, the total emission over the
31 period was not strongly sensitive to a change of $\pm 10\%$ (± 0.08 mm) (Table 6). This is a result of
32 the model features that 1) allow only a $(\Delta z \times (\theta_{fc} - \theta_{pwp})) = 1.2$ mm of maximum liquid content

1 in the model soil pore and 2) do not allow wash out TAN from the source layer. Therefore, in
2 the GAG model even a heavy rain event ($> 6\text{ mm / hr}$) - apart from the slight effect on
3 evaporation – has the same effect as a modest 1.2 mm / hr of precipitation. In the test simulation
4 during the rain event the soil reached its maximum water content (θ_{fc}). We found that by
5 decreasing the amount of total precipitation so that the soil does not reach θ_{fc} , the maximum
6 difference in total emission was +3%.

7 In addition, the timing of the rain event can also lead to a difference in total NH_3 emission due
8 to the associated increase in R_{soil} which tends to suppress the rate of volatilization. We found
9 that the timing of the rain event affects the NH_3 emission, with up to a 6% reduction or 2%
10 increase in the total NH_3 emission (see the model results in Section S5). Nevertheless, it must
11 be emphasized that in reality NH_3 can escape from wet soil not only through gaseous diffusion
12 in the empty soil pores. Dissolved NH_3 may get to the soil surface also through the solution and
13 can be volatilized from there (Cooter et al., 2010). This is not taken into account in the present
14 soil resistance parametrisation. Therefore, the effect of rainfall might not be as strong as this
15 experiment showed. On the other hand, as we mentioned earlier, during a dry period urea
16 hydrolysis may slow or stop in absence of water. If the rainfall begins after such a dry period,
17 by restarting urea hydrolysis, it can even enhance ammonia emission rather than suppress it.

18

19 **7 Discussion**

20 We constructed a novel NH_3 emission model for a urine patch (GAG) that is capable of
21 simulating the TAN and the water content of the soil under a urine patch and also soil pH. The
22 difference between the simulated and measured values suggested that to improve the model,
23 further investigation is needed regarding the effect of a possible restart of urea hydrolysis with
24 rain events.

25 The sensitivity analysis to the uncertain parameters showed that soil resistance had more than
26 an order of magnitude stronger effect on soil NH_3 emission than the atmospheric resistances.
27 An exceptional case is when weak wind is coupled with dry soil, in which case atmospheric
28 and soil resistances may become comparable.

29 Our sensitivity analysis also showed that if the thickness of the source layer (Δz) is modified
30 by a given percentage, the difference in the resulting total ammonia emission over the modelling
31 period will be half of this percentage. Therefore, this source of error must be considered when

1 model results are evaluated. Future work should also consider how independent datasets can
2 help characterize the depth of the effective soil emission layer, as well as consider how both
3 downward and upward migration of TAN with deeper soil layers can be addressed.

4 In the case of pH we showed that process-based modelling of pH is necessary to reproduce the
5 very first high peak in NH_3 emission. The simulations were carried out with an assumed soil
6 buffering capacity. While this affects the timing of emissions, we found that the total emission
7 is not sensitive to the value of β and it is able to represent the main temporal development of
8 ammonia emission even with 0 buffering capacity.

9 On the other hand, we found that incorporating a simple estimation of CO_2 emission allows the
10 model to reproduce the measured soil pH values more accurately than neglecting CO_2
11 emissions. Future work should therefore consider how CO_2 fluxes could be incorporated more
12 systematically into the GAG model.

13 The model turned out to be sensitive to the value of soil water content at field capacity (θ_{fc}) and
14 at permanent wilting point (θ_{pwp}). Thus, at regional scale application, where mostly
15 recommended values of these parameters are available, this error has to be considered when
16 interpreting the model results.

17 Our results support the vital role of temperature in NH_3 exchange, showing a high correlation
18 with the temperature parameters as well as strong sensitivity to them. Nevertheless, the GAG
19 model provides only a modest overall temperature dependence in total NH_3 emission compared
20 to what was reported in the literature earlier. A possible explanation for this is that, according
21 to our results, the sensitivity to temperature is higher close to urine application than in the later
22 stages and may depend also on interactions with other nitrogen cycling processes.

23 In addition, we found that wind speed and relative humidity are also significant influencing
24 factors. In the case of RH we observed a dual effect through its effect on the modelled soil
25 evaporation and the modelled deposition to leaf surfaces, with the latter being the dominant
26 term for the present simulations.

27 In contrast to the NH_3 volatilization models published earlier for urea affected soils (Sherlock
28 and Goh, 1985; Rachhpal and Nye, 1986), our model, incorporating a canopy compensation
29 point model, accounts for the effect of the meteorological parameters on net canopy exchange
30 of NH_3 . Compared with the model constructed by Laubach et al. (2012), GAG is capable of
31 simulating the influence of vegetation on NH_3 exchange. In addition, our model also simulates

1 soil pH, the TAN and the water content of the soil, allowing it to predict net NH_3 emission,
2 instead of operating only in “inverse” mode, calculating soil parameters based on flux
3 measurements.

4 Rachhpal and Nye (1986) suggested a solution for dynamic modelling of soil pH with a set of
5 continuity equations. However, in their approach the dissociation coefficients, as well as the
6 urea hydrolysis rate, were independent of temperature. Even though the GAG model accounts
7 for the same chemical reactions, it incorporates a different mathematical description and
8 accounts for the missing temperature dependencies.

9 Dynamic simulation of soil pH is novel among the NH_3 exchange models on the ecosystem
10 scale. In the PaSim ecosystem model (Riedo et al., 2002) pH is treated as a constant, and the
11 same is true for the VOLT’AIR model (Génermont and Cellier, 1997) developed for simulating
12 NH_3 emission related to fertilizer and manure application. Furthermore, the framework of GAG
13 is simpler and requires less input data than the VOLT’AIR model. Therefore, for grazing
14 situations, it is much easier to adapt GAG on both field and regional scale.

15 As our final goal is to apply the model to regional scale, simplicity was a key aspect of the
16 model development, avoiding extra steps of model simplification in the later stages of our
17 project. Therefore, the model operates with a single layer approach in the soil. Although this is
18 a simpler approach compared to the some of the above mentioned models (Rachhpal and Nye,
19 1986, Génermont and Cellier, 1997 and Riedo et al., 2002), the model code is easily amendable,
20 which enables to add new modules to GAG in the future.

21 Since all the input parameters can be obtained for larger scales, considering the possible errors,
22 GAG is concluded to be suitable for larger scale application, such as in regional atmospheric
23 and ecosystem models. In addition, as it is dynamically driven by weather parameters, it can
24 serve as a base for further studies of climate dependency of ammonia emission from grazed
25 fields on both plot and regional scale.

26

27 **8 Conclusions**

28 We report the description of a process-based, weather-driven ammonia exchange model for a
29 urine patch that is capable of simulating the TAN and the water content of the soil under a urine
30 patch and also soil pH.

1 The model tests suggest that ammonia volatilization from a urine patch can be affected by the
2 possible restart of urea hydrolysis after a rain event as well as CO₂ emission from the soil.

3 The vital role of temperature in NH₃ exchange is supported by our model results; however, the
4 GAG model provides only a modest overall temperature dependence in total NH₃ emission
5 compared with the literature. This, according to our findings, can be explained by the higher
6 sensitivity to temperature close to urine application than in the later stages and may depend on
7 interactions with other nitrogen cycling processes. In addition, we found that wind speed and
8 relative humidity are also significant influencing factors. These relationships need to be further
9 tested in relation to field measurements.

10 For simplicity, to allow subsequent regional upscaling, the model operates with a single soil
11 layer approach, neglecting water movement and solution mixing in the soil. Although this is a
12 limitation of the current model version, the model code is easily amendable, which facilitates
13 to add new modules to GAG in the future.

14 Considering that all the input parameters can be obtained for larger scales, GAG is potentially
15 suitable for field and regional scale application, serving as a tool for further investigation of the
16 effects of climate change on ammonia emissions and deposition.

17

18 **Acknowledgements**

19 This work was carried out within the framework of the ÉCLAIRE project (Effects of Climate
20 Change on Air Pollution and Response Strategies for European Ecosystems) funded by the EU's
21 Seventh Framework Programme for Research and Technological Development (FP7).

22

23 **Abbreviations**

Abbreviation (unit)	Model variable
$\frac{D_{O_3}}{D_{NH_3}}$	Ratio of diffusivity of O ₃ and NH ₃
[X] (mol dm ⁻³)	Concentration of compound X
a	Parameter for calculating R _w
A _h	Parameter for urea hydrolysis simulation

A_{patch} (m ²)	Area of a urine patch
B_C (mol)	Carbon content of the source layer (originating from urea)
$B_{\text{H}_2\text{O}}$ (dm ³)	Water budget in the source layer
$B_{\text{H}_2\text{O}(\text{max})}$ (dm ³)	Maximal water amount in the source layer
$B_{\text{H}_2\text{O}(\text{min})}$ (dm ³)	Minimal water amount in the source layer
$B_{\text{H}_2\text{O}}'$ (dm ³)	Precalculated water budget in the source layer
$B_{\text{H}_2\text{O}}^{\text{Tot}}$ (dm ³)	Total water budget under a urine patch
B_N (mol)	TAN + gaseous ammonia content in the source layer
B_{TAN} (g N)	TAN budget in the source layer
B_{urea} (g N)	Urea budget under a urine patch
B_X (mol) (X= H ₂ CO ₃ , HCO ₃ ⁻ , CO ₃ ²⁻ , CO _{2(g)} , NH ₄ ⁺ , NH _{3(aq)} , NH _{3(g)} , H ⁺)	Budget of a chemical compound X under the urine patch
C_d	Effect of day and night on evapotranspiration
c_N (N dm ⁻³)	N content of the urine
c_N^{Tot} (g N dm ⁻³)	Urine N content after dilution in the soil
D_g (m ² s ⁻¹)	Diffusivity of NH ₃ in air
E (mm h ⁻¹)	Soil evaporation rate
e_a (kPa)	Actual water vapour pressure
e_s (kPa)	Saturated water vapour pressure
ET (mm h ⁻¹)	Actual evapotranspiration rate
ET_0 (mm h ⁻¹)	Reference evapotranspiration rate
f_c (m ² m ⁻²)	Vegetation coverage
F_f (μg N m ⁻² s ⁻¹)	NH ₃ exchange flux with the foliage

F_g ($\mu\text{g N m}^{-2} \text{s}^{-1}$)	NH ₃ exchange flux over the ground
F_{sto} ($\mu\text{g N m}^{-2} \text{s}^{-1}$)	NH ₃ exchange flux with stomata
F_t ($\mu\text{g N m}^{-2} \text{s}^{-1}$)	Total NH ₃ exchange flux over the canopy
f_w ($\text{m}^2 \text{m}^{-2}$)	Wetted uncovered soil fraction
F_w ($\mu\text{g N m}^{-2} \text{s}^{-1}$)	NH ₃ deposition flux to water and waxes on the leaf surface
G ($\text{MJ m}^2 \text{h}^{-1}$)	Soil heat flux
g_{light}	Relative conductance for the effect of light on g_s
g_{max} ($\text{mmol O}_3 \text{m}^{-2}$)	Maximal stomatal conductance
g_{min}	Minimal relative stomatal conductance
g_{pot}	Relative stomatal conductance for the effect of plant phenological state on g_s
g_s ($\text{mmol O}_3 \text{m}^{-2}$)	Stomatal conductance for O ₃
g_{SWP}	Relative conductance for the effect of soil water on g_s
g_{temp}	Relative conductance for the effect of temperature on g_s
g_{VPD}	Relative conductance for the effect of vapour pressure deficit on g_s
$H(X)$ ($\text{mol dm}^{-3} (\text{mol dm}^{-3})^{-1}$)	Henry coefficient for the given gas X
i_C (mol)	Carbon input to the urine patch
i_N (mol)	TAN input to the urine patch (TAN production in moles)
$K(X)$ (mol dm^{-3})	Dissociation constant for the given compound X
K_c	Crop coefficient
K_{cb}	Transpiration coefficient
K_e	Soil evaporation coefficient

k_h	Urea hydrolysis constant
L (m)	Monin-Obukhov length
LAI ($m^2 m^{-2}$)	Leaf area index
N_{app} ($kg N ha^{-1}$)	Nitrogen applied over a urine patch
N_{prod} (g N)	TAN production
P (mm)	Precipitation
PAR ($\mu mol m^2 s^{-1}$)	Photosynthetically active radiation
R_a ($s m^{-1}$)	Aerodynamic resistance over the canopy
R_{ac} ($s m^{-1}$)	Aerodynamic resistance in the canopy
R_b ($s m^{-1}$)	Resistance of the quasi-laminar layer over the canopy
R_{bg} ($s m^{-1}$)	Resistance of the quasi-laminar layer in the canopy
REW (mm)	Readily evaporable water in the soil
R_{glob} ($MJ m^2 h^{-1}$)	Global radiation / solar radiation
RH (%)	Relative humidity
R_n ($MJ m^2 h^{-1}$)	Net radiation
r_{RX} (mol)	Consumption or production of a given compound in reaction X.
R_{soil} ($s m^{-1}$)	Soil resistance
R_{sto} ($s m^{-1}$)	Stomatal resistance
$R_{sto}(O_3)$ ($s m^{-1}$)	Stomatal resistance for O_3
R_w ($s m^{-1}$)	Cuticular resistance
$R_w(min)$ ($s m^{-1}$)	Minimal cuticular resistance
S_{MI}	Soil moisture index
T ($^{\circ}C$)	Air temperature at 2 m
t_i	ith time step

T_{soil} (°C)	Soil temperature
u (m s ⁻¹)	Wind speed
u^* (m s ⁻¹)	Friction velocity
u^*_{g}	Friction velocity at ground level in the canopy
U_{add} (g N)	Urea added to the source layer
V_{air} (dm ³)	Volume of the air in the source layer
W_{evap} (dm ³)	Water loss as soil evaporation from the urine patch
W_{rain} (dm ³)	Water input as rain water over the urine patch
W_{urine} (dm ³)	Volume of urine
z_1 (m)	Height of the top of logarithmic wind profile
z_w (m)	Height of wind measurement
α	Parameter for calculating R_{ac}
β (mol H ⁺ (pH unit) ⁻¹ dm ⁻³)	Soil buffering capacity
β_{patch} (mol H ⁺ (pH unit) ⁻¹)	Buffering capacity of the source layer
γ (kPa °C ⁻¹)	Psychometric constant
Γ_p	NH ₃ emission potential in the soil pore
Γ_{sto}	NH ₃ emission potential from the stomata
$\Gamma_{\text{sto}}(\text{max})$	Maximal NH ₃ emission potential from the stomata
Δ (kPa °C ⁻¹)	Slope of saturation vapour pressure curve
Δz (mm)	Thickness of the source layer
Δz_E (m)	Thickness of the evaporation layer
θ (m ³ m ⁻³)	Volumetric water content
θ_{fc} (m ³ m ⁻³)	Field capacity
θ_{por} (m ³ m ⁻³)	Porosity
θ_{pwp} (m ³ m ⁻³)	Permanent wilting point

ξ	Soil tortuosity
τ (days)	Decay parameter
χ_a ($\mu\text{g N m}^{-3}$)	Air concentration of NH_3
χ_c ($\mu\text{g N m}^{-3}$)	Compensation point above the vegetation
χ_p ($\mu\text{g N m}^{-3}$)	Compensation point in the soil pores
χ_{sto} ($\mu\text{g N m}^{-3}$)	Stomatal compensation point
χ_{z0} ($\mu\text{g N m}^{-3}$)	Canopy compensation point

1

2 **References**

- 3 Allen, R. G., Pereira, L. S., Raes, D. and Smith, M.: Crop evapotranspiration-Guidelines for
4 computing crop water requirements, FAO Irrigation and drainage paper 56, FAO, Rome, Italy,
5 1998.
- 6 Bates, R. G. and Pinching, G. D.: Acidic dissociation constant of ammonium ion at 0-degrees-
7 C to 50-degrees-C, and the base strength of ammonia, J. Res. Nat. Bur. Stand., 42, 419-430,
8 doi:10.6028/jres.042.037, 1949.
- 9 Betteridge, K., Andrewes, W. G. K. and Sedcole, J. R.: Intake and excretion of nitrogen,
10 potassium and phosphorus by grazing steers, J Agr Sci, 106, 393-404, 1986.
- 11 Burkhardt, J., Kaiser, H., Goldbach, H. and Kappen, L.: Measurements of electrical leaf surface
12 conductance reveal re-condensation of transpired water vapour on leaf surfaces, Plant, Cell
13 Environ., 22, 189-196, doi:10.1046/j.1365-3040.1999.00387.x, 1999.
- 14 Burkhardt, J., Flechard, C. R., Gresens, F., Mattsson, M., Jongejan, P. A. C., Erisman, J. W.,
15 Weidinger, T., Meszaros, R., Nemitz, E. and Sutton, M. A.: Modelling the dynamic chemical
16 interactions of atmospheric ammonia with leaf surface wetness in a managed grassland canopy,
17 Biogeosciences, 6, 67-84, doi:10.5194/bg-6-67-2009, 2009.
- 18 Cooter, E. J., Bash, J. O., Walker, J. T., Jones, M. R. and Robarge, W.: Estimation of NH_3 bi-
19 directional flux from managed agricultural soils, Atmos. Environ., 44, 2107-2115,
20 10.1016/j.atmosenv.2010.02.044, 2010.

1 Dasgupta, P. K. and Dong, S.: Solubility of ammonia in liquid water and generation of trace
2 levels of standard gaseous ammonia, *Atmos. Environ.*, 20, 565-570, doi:10.1016/0004-
3 6981(86)90099-5, 1986.

4 Dijkstra, J., Oenema, O., van Groenigen, J. W., Spek, J. W., van Vuuren, A. M. and Bannink,
5 A.: Diet effects on urine composition of cattle and N₂O emissions, *animal*, 7, 292-302,
6 doi:10.1017/S1751731113000578, 2013.

7 Doak, B. W.: Some chemical changes in the nitrogenous constituents of urine when voided on
8 pasture, *J Agr Sci*, 42, 162-171, 1952.

9 EDGAR: Emissions Database for Global Atmospheric Research v4.2,
10 <http://edgar.jrc.ec.europa.eu/>, last access: 20 May 2014, 2011.

11 Emberson, L., Simpson, D., Tuovinen, J.-P., Ashmore, M. and Cambridge, H.: Towards a
12 model of ozone deposition and stomatal uptake over Europe, EMEP MSC-W Note 6/2000, The
13 Norwegian Meteorological Institute, Oslo, Norway, 2000.

14 Farquhar, G. D., Firth, P. M., Wetselaar, R. and Weir, B.: On the Gaseous Exchange of
15 Ammonia between Leaves and the Environment: Determination of the Ammonia
16 Compensation Point, *Plant. Physiol.*, 66, 710-714, doi:10.1104/pp.66.4.710, 1980.

17 Flechard, C. R., Fowler, D., Sutton, M. A. and Cape, J. N.: A dynamic chemical model of bi-
18 directional ammonia exchange between semi-natural vegetation and the atmosphere, *Q. J. Roy.*
19 *Meteor. Soc.*, 125, 2611-2641, doi:10.1002/qj.49712555914, 1999.

20 Flechard, C. R., Massad, R. S., Loubet, B., Personne, E., Simpson, D., Bash, J. O., Cooter, E.
21 J., Nemitz, E. and Sutton, M. A.: Advances in understanding, models and parameterizations of
22 biosphere-atmosphere ammonia exchange, *Biogeosciences*, 10, 5183-5225, doi:10.5194/bg-10-
23 5183-2013, 2013.

24 Fowler, D., Coyle, M., Skiba, U., Sutton, M. A., Cape, J. N., Reis, S., Sheppard, L. J., Jenkins,
25 A., Grizzetti, B., Galloway, J. N., Vitousek, P., Leach, A., Bouwman, A. F., Butterbach-Bahl,
26 K., Dentener, F., Stevenson, D., Amann, M. and Voss, M.: The global nitrogen cycle in the
27 twenty-first century, *Philos. T. R. Soc. B*, 368, 20130164, doi:10.1098/rstb.2013.0164, 2013.

28 Galloway, J. N., Townsend, A. R., Erisman, J. W., Bekunda, M., Cai, Z., Freney, J. R.,
29 Martinelli, L. A., Seitzinger, S. P. and Sutton, M. A.: Transformation of the Nitrogen Cycle:

1 Recent Trends, Questions, and Potential Solutions, *Science*, 320, 889-892,
2 doi:10.1126/science.1136674, 2008.

3 Générmont, S. and Cellier, P.: A mechanistic model for estimating ammonia volatilization from
4 slurry applied to bare soil, *Agr. Forest Meteorol.*, 88, 145-167, doi:10.1016/S0168-
5 1923(97)00044-0, 1997.

6 Harned, H. S. and Davis, R.: The Ionization Constant of Carbonic Acid in Water and the
7 Solubility of Carbon Dioxide in Water and Aqueous Salt Solutions from 0 to 50°, *J. Am. Chem.*
8 *Soc.*, 65, 2030-2037, doi:10.1021/ja01250a059, 1943.

9 Harned, H. S. and Scholes, S. R.: The Ionization Constant of HCO_3^- from 0 to 50°, *J. Am.*
10 *Chem. Soc.*, 63, 1706-1709, doi:10.1021/ja01851a058, 1941.

11 Hellsten, S., Dragosits, U., Place, C. J., Vieno, M., Dore, A. J., Misselbrook, T. H., Tang, Y. S.
12 and Sutton, M. A.: Modelling the spatial distribution of ammonia emissions in the UK, *Environ.*
13 *Pollut.*, 154, 370-379, doi:10.1016/j.envpol.2008.02.017, 2008.

14 Hicks, B. B., Baldocchi, D. D., Meyers, T. P., Hosker, R. P., Jr. and Matt, D. R.: A preliminary
15 multiple resistance routine for deriving dry deposition velocities from measured quantities,
16 *Water Air Soil Pollut.*, 36, 311-330, doi:10.1007/BF00229675, 1987.

17 Hoogendoorn, C. J., Betteridge, K., Costall, D. A. and Ledgard, S. F.: Nitrogen concentration
18 in the urine of cattle, sheep and deer grazing a common ryegrass/cocksfoot/white clover pasture,
19 *New Zeal. J. Agr. Res.*, 53, 235-243, doi:10.1080/00288233.2010.499899, 2010.

20 Horváth, L., Asztalos, M., Führer, E., Mészáros, R. and Weidinger, T.: Measurement of
21 ammonia exchange over grassland in the Hungarian Great Plain, *Agr. Forest Meteorol.*, 130,
22 282-298, doi:10.1016/j.agrformet.2005.04.005, 2005.

23 Kielland, J.: Individual Activity Coefficients of Ions in Aqueous Solutions, *J. Am. Chem. Soc.*, 59,
24 1675-1678, doi:10.1021/ja01288a032 1937.

25 Laubach, J., Taghizadeh-Toosi, A., Gibbs, S. J., Sherlock, R. R., Kelliher, F. M. and Grover, S.
26 P. P.: Ammonia emissions from cattle urine and dung excreted on pasture, *Biogeosciences*, 10,
27 327-338, doi:10.5194/bg-10-327-2013, 2013.

28 Laubach, J., Taghizadeh-Toosi, A., Sherlock, R. R. and Kelliher, F. M.: Measuring and
29 modelling ammonia emissions from a regular pattern of cattle urine patches, *Agr. Forest*
30 *Meteorol.*, 156, 1-17, doi:10.1016/j.agrformet.2011.12.007, 2012.

1 Leuning, R., Freney, J. R., Denmead, O. T. and Simpson, J. R.: A sampler for measuring
2 atmospheric ammonia flux, *Atmos. Environ.*, 19, 1117-1124, doi:10.1016/0004-
3 6981(85)90196-9, 1985.

4 Lin, X., Wang, S., Ma, X., Xu, G., Luo, C., Li, Y., Jiang, G. and Xie, Z.: Fluxes of CO₂, CH₄,
5 and N₂O in an alpine meadow affected by yak excreta on the Qinghai-Tibetan plateau during
6 summer grazing periods, *Soil Biol. Biochem.*, 41, 718-725, doi:10.1016/j.soilbio.2009.01.007,
7 2009.

8 Ma, X., Wang, S., Wang, Y., Jiang, G. and Nyren, P.: Short-term effects of sheep excrement
9 on carbon dioxide, nitrous oxide and methane fluxes in typical grassland of Inner Mongolia,
10 *New Zeal. J. Agr. Res.*, 49, 285-297, 2006.

11 Massad, R.-S., Tuzet, A., Loubet, B., Perrier, A. and Cellier, P.: Model of stomatal ammonia
12 compensation point (STAMP) in relation to the plant nitrogen and carbon metabolisms and
13 environmental conditions, *Ecol. Model.*, 221, 479-494, doi:10.1016/j.ecolmodel.2009.10.029,
14 2010a.

15 Massad, R. S., Nemitz, E. and Sutton, M. A.: Review and parameterisation of bi-directional
16 ammonia exchange between vegetation and the atmosphere, *Atmos. Chem. Phys.*, 10, 10359-
17 10386, doi:10.5194/acp-10-10359-2010, 2010b.

18 Millington, R. J. and Quirk, J. P.: Permeability of porous solids, *T. Faraday Soc.*, 57, 1200-
19 1207, doi:10.1039/tf9615701200, 1961.

20 Misselbrook, T. H., Gilhespy, S. L., Cardenas, L. M., Chambers, B. J., Smith, K. A., Williams,
21 J. and Dragosits, U.: Inventory of Ammonia Emissions from UK Agriculture, Inventory
22 Submission Report, DEFRA, London, UK, 2012.

23 Nemitz, E., Milford, C. and Sutton, M. A.: A two-layer canopy compensation point model for
24 describing bi-directional biosphere-atmosphere exchange of ammonia, *Q. J. Roy. Meteor. Soc.*,
25 127, 815-833, doi:10.1256/smsqj.57305, 2001.

26 Nemitz, E., Sutton, M. A., Schjoerring, J. K., Husted, S. and Paul Wyers, G.: Resistance
27 modelling of ammonia exchange over oilseed rape, *Agr. Forest Meteorol.*, 105, 405-425,
28 doi:10.1016/S0168-1923(00)00206-9, 2000.

29 NIWA: The National Climate Database, <http://cliflo.niwa.co.nz/>, last access: 2 December 2013,
30 2015.

1 Petersen, S. O., Sommer, S. G., Aaes, O. and Sjøgaard, K.: Ammonia losses from urine and
2 dung of grazing cattle: effect of N intake, *Atmos. Environ.*, 32, 295-300, doi:10.1016/S1352-
3 2310(97)00043-5, 1998.

4 R Core Team: R: A language and environment for statistical computing. R Foundation for
5 Statistical Computing, Vienna, Austria, 2012.

6 Rachhpal, S. and Nye, P. H.: A model of ammonia volatilization from applied urea. I.
7 Development of the model, *J. Soil Sci.*, 37, 9-20, doi:10.1111/j.1365-2389.1986.tb00002.x,
8 1986.

9 Riddick, S. N.: Global ammonia emissions from seabird colonies, Ph.D. thesis, Kings College,
10 London, UK, 2012.

11 Riedo, M., Milford, C., Schmid, M. and Sutton, M. A.: Coupling soil–plant–atmosphere
12 exchange of ammonia with ecosystem functioning in grasslands, *Ecol. Model.*, 158, 83-110,
13 doi:10.1016/S0304-3800(02)00169-2, 2002.

14 Sherlock, R. R. and Goh, K. M.: Dynamics of ammonia volatilization from simulated urine
15 patches and aqueous urea applied to pasture I. Field experiments, *Fert. Res.*, 5, 181-195,
16 doi:10.1007/BF01052715, 1984.

17 Sherlock, R. R. and Goh, K. M.: Dynamics of ammonia volatilization from simulated urine
18 patches and aqueous urea applied to pasture. II. Theoretical derivation of a simplified model,
19 *Fert. Res.*, 6, 3-22, doi:10.1007/BF01058161, 1985.

20 Shorten, P. R. and Pleasants, A. B.: A stochastic model of urinary nitrogen and water flow in
21 grassland soil in New Zealand, *Agric., Ecosyst. Environ.*, 120, 145-152,
22 doi:10.1016/j.agee.2006.08.017, 2007.

23 Simpson, D., Benedictow, A., Berge, H., Bergström, R., Emberson, L. D., Fagerli, H., Flechard,
24 C. R., Hayman, G. D., Gauss, M., Jonson, J. E., Jenkin, M. E., Nyíri, A., Richter, C., Semeena,
25 V. S., Tsyro, S., Tuovinen, J. P., Valdebenito, Á. and Wind, P.: The EMEP MSC-W chemical
26 transport model; technical description, *Atmos. Chem. Phys.*, 12, 7825-7865, doi:10.5194/acp-
27 12-7825-2012, 2012.

28 Sutton, M. A. and Fowler, D.: A model for inferring bi-directional fluxes of ammonia over plant
29 canopies, in: WMO Conference on the Measurement and Modeling of Atmospheric
30 Composition Changes including Pollution Transport. WMO/GAW-91, Sofia, Bulgaria, 04–08
31 October 1993, WMO, Geneva, 179-182, 1993.

1 Sutton, M. A., Howard, C. M., Erisman, J. W., Bealey, W. J., Billen, G., Bleeker, A., Bouwman,
2 A. F., Grennfelt, P., van Grinsven, H. and Grizzetti, B.: The challenge to integrate nitrogen
3 science and policies: the European Nitrogen Assessment approach, in: The European Nitrogen
4 Assessment: Sources, Effects and Policy Perspectives, Sutton, M. A., Howard, C. M., Erisman,
5 J. W., Billen, G., Bleeker, A., Grennfelt, P., Van Grinsven, H. & Grizzetti, B. (Eds.), Cambridge
6 University Press, Cambridge, UK, 82-96, 2011.

7 Sutton, M. A., Reis, S., Riddick, S. N., Dragosits, U., Nemitz, E., Theobald, M. R., Tang, Y.
8 S., Braban, C. F., Vieno, M., Dore, A. J., Mitchell, R. F., Wanless, S., Daunt, F., Fowler, D.,
9 Blackall, T. D., Milford, C., Flechard, C. R., Loubet, B., Massad, R., Cellier, P., Personne, E.,
10 Coheur, P. F., Clarisse, L., Van Damme, M., Ngadi, Y., Clerbaux, C., Skjøth, C. A., Geels, C.,
11 Hertel, O., Wichink Kruit, R. J., Pinder, R. W., Bash, J. O., Walker, J. T., Simpson, D., Horváth,
12 L., Misselbrook, T. H., Bleeker, A., Dentener, F. and de Vries, W.: Towards a climate-
13 dependent paradigm of ammonia emission and deposition, *Philos. T. R. Soc. B*, 368, 20130166,
14 doi:10.1098/rstb.2013.0166, 2013.

15 Sutton, M. A., Schjorring, J. K. and Wyers, G. P.: Plant-Atmosphere Exchange of Ammonia
16 *Philos. T. R. Soc. A*, 351, 261-276, doi:10.1098/rsta.1995.0033, 1995.

17 Vieno, M., Dore, A. J., Stevenson, D. S., Doherty, R., Heal, M. R., Reis, S., Hallsworth, S.,
18 Tarrason, L., Wind, P., Fowler, D., Simpson, D. and Sutton, M. A.: Modelling surface ozone
19 during the 2003 heat-wave in the UK, *Atmos. Chem. Phys.*, 10, 7963-7978, doi:10.5194/acp-
20 10-7963-2010, 2010.

21 Vieno, M., Heal, M. R., Hallsworth, S., Famulari, D., Doherty, R. M., Dore, A. J., Tang, Y. S.,
22 Braban, C. F., Leaver, D., Sutton, M. A. and Reis, S.: The role of long-range transport and
23 domestic emissions in determining atmospheric secondary inorganic particle concentrations
24 across the UK, *Atmos. Chem. Phys.*, 14, 8435-8447, doi:10.5194/acp-14-8435-2014, 2014.

25 Walter, I., Allen, R., Elliott, R., Jensen, M., Itenfisu, D., Mecham, B., Howell, T., Snyder, R.,
26 Brown, P., Echings, S., Spofford, T., Hattendorf, M., Cuenca, R., Wright, J. and Martin, D.:
27 ASCE's Standardized Reference Evapotranspiration Equation, in: *Watershed Management and*
28 *Operations Management 2000*, American Society of Civil Engineers, Fort Collins, Colorado,
29 US, 20–24 June 2000, 1-11, 2001.

- 1 Wang, X., Huang, D., Zhang, Y., Chen, W., Wang, C., Yang, X. and Luo, W.: Dynamic changes
2 of CH₄ and CO₂ emission from grazing sheep urine and dung patches in typical steppe, *Atmos.*
3 *Environ.*, 79, 576-581, doi:10.1016/j.atmosenv.2013.07.003, 2013.
- 4 Whitehead, D. C., Lockyer, D. R. and Raistrick, N.: Volatilization of ammonia from urea
5 applied to soil: Influence of hippuric acid and other constituents of livestock urine, *Soil Biol.*
6 *Biochem.*, 21, 803-808, doi:10.1016/0038-0717(89)90174-0, 1989.
- 7 Whitehead, D. C. and Raistrick, N.: The volatilization of ammonia from cattle urine applied to
8 soils as influenced by soil properties, *Plant Soil*, 148, 43-51, doi:10.1007/BF02185383, 1993.
- 9 Wilhelm, E., Battino, R. and Wilcock, R. J.: Low-pressure solubility of gases in liquid water,
10 *Chem. Rev.*, 77, 219-262, doi:10.1021/cr60306a003, 1977.
- 11 Wu, Y., Walker, J., Schwede, D., Peterslidard, C., Dennis, R. and Robarge, W.: A new model
12 of bi-directional ammonia exchange between the atmosphere and biosphere: Ammonia stomatal
13 compensation point, *Agr. Forest Meteorol.*, 149, 263-280,
14 doi:10.1016/j.agrformet.2008.08.012, 2009.

1 Table 1. Chemical equations – indicated by R0-5 - simulated within the model, (where applicable) their equilibrium coefficient according to
 2 definition (K for dissociation and H for dissolution) and the coefficients expressed as the function of soil temperature (T_{soil} (K)) and their
 3 references (squared brackets denotes that the concentration of every compound is in mol dm^{-3}).
 4

Chemical equation	Equilibrium coefficient	Equilibrium coefficient as a function of temperature	Reference
R0: $CO(NH_2)_2 + 2H_2O + H^+ \rightarrow 2NH_4^+ + HCO_3^-$	-	-	-
R1: $NH_4^+ \Leftrightarrow NH_{3(aq)} + H^+$	$K(NH_4^+) = \frac{[NH_{3(aq)}][H^+]}{[NH_4^+]}$	$K(NH_4^+) = 5.67 \times 10^{-10} \exp\left(-6286\left(\frac{1}{T_{soil}} - \frac{1}{298.15}\right)\right)$	Bates and Pinching, 1949
R2: $HCO_3^- \Leftrightarrow CO_3^{2-} + H^+$	$K(HCO_3^-) = \frac{[H^+][CO_3^{2-}]}{[HCO_3^-]}$	$\lg(K(X)) = -\left(\left(\frac{a}{T_{soil}}\right) + (b \times T_{soil}) - c\right)$ a=2902.39 b=0.02379 c=6.4980	Harned and Scholes, 1941
R3: $H_2CO_3 \Leftrightarrow HCO_3^- + H^+$	$K(H_2CO_3) = \frac{[HCO_3^-][H^+]}{[H_2CO_3]}$	$\lg(K(X)) = -\left(\left(\frac{a}{T_{soil}}\right) + (b \times T_{soil}) - c\right)$ a=3404.71 b=0.032786 c=14.8435	Harned and Davis, 1943
R4: $NH_{3(aq)} \Leftrightarrow NH_{3(g)}$	$H(NH_{3(g)}) = \frac{[NH_{3(aq)}]}{[NH_{3(g)}]}$	$H(NH_{3(g)}) = 56 \times \exp\left(4092 \times \left(\frac{1}{T_{soil}} - \frac{1}{298.15}\right)\right) \times c_{con}$	Dasgupta and Dong, 1986
R5: $H_2CO_3 \Leftrightarrow CO_{2(g)}$	$H(CO_{2(g)}) = \frac{[H_2CO_3]}{[CO_{2(g)}]}$	$H(CO_{2(g)}) = 0.034 \times \exp\left(2400 \times \left(\frac{1}{T_{soil}} - \frac{1}{298.15}\right)\right) \times c_{con}$ (where $c_{con} = \left(\frac{0.001 \frac{m^3}{dm^3} \times 1.013 \times 10^5 \frac{Pa}{atm}}{8.314 \frac{J}{Kmol} T_{soil}}\right)^{-1}$ is the conversion from $\text{atm} (\text{mol dm}^{-3})^{-1}$ to $(\text{mol dm}^{-3}) (\text{mol dm}^{-3})^{-1}$)	Wilhelm et al., 1977

5

1 Table 2. Urine patch details from the experiment of Laubach et al. (2012) (or from other sources
 2 as listed in the footnote) and site specific model constants.

Model constants	Value
Urine patch specific constants	
A_{patch} (area of a urine patch) ¹	0.25 m ²
c_{N} (N content of the urine)	10 g N dm ⁻³
W_{urine} (volume of urine)	1.5 dm ³
Δz (thickness of the source layer) ²	4 mm
k_{h} (urea hydrolysis constant) ³	0.23
Site specific constants	
Longitude	172 ⁰ 27.34'E
Latitude	43 ⁰ 38.56'S
Height above sea level	11 m
θ_{pwp} (permanent wilting point) ⁴	0.1
θ_{fc} (field capacity) ⁴	0.4
θ_{por} (porosity)	0.62
f_{c} (vegetation coverage)	35%
z_{w} (height of wind measurement)	2.1 m

3 ¹ In the experiment the expansion of the patches was observed up to 0.5 m². For model
 4 sensitivity to A_{patch} see Section 5.2.

5 ² Assumed in this study.

6 ³ For summer (Sherlock and Goh, 1984)

7 ⁴ Assumed based on the provided measured volumetric water content dataset.

8

- 1 Table 3. Measured data used as input and the base of comparison with the model results,
 2 together with their original time resolution and their conversion to hourly time resolution.

Variable	Original time resolution	Adaptation to hourly time resolution
Input data		
χ_a ($\mu\text{g N m}^{-3}$)	Various (2-10 hourly)	Interpolated for the required hours.
u (m s^{-1}) – at 2.1 m		
PAR ($\mu\text{mol m}^{-2} \text{s}^{-1}$)		
T_{soil} ($^{\circ}\text{C}$) - at 2 cm	Half hourly	Averaged for the given hour.
p (kPa)		
H ($\text{MJ m}^{-2} \text{h}^{-1}$)		
P (mm)	Half hourly	Summed up for the given hour.
T ($^{\circ}\text{C}$) - at 3.85 m	Half hourly	Averaged for the given hour then calculated to 2 m height considering the average temperature gradient $6.5 \text{ }^{\circ}\text{C}/\text{km}$: $T(2\text{m})=T(3.85\text{m})-0.0065 \times 1.85$
R_{glob} ($\text{MJ m}^{-2} \text{h}^{-1}$)*	Hourly	-
RH (%)*		
Data used in the comparison		
F_t ($\mu\text{g N m}^{-2} \text{s}^{-1}$)	Various (2-10 hourly)	Measurements in the midpoints of the collection periods were considered as representative hourly averages.
θ ($\text{m}^3 \text{m}^{-3}$)		

pH	Various	Measurements in the given hour
NH _x -N (µg N (g soil) ⁻¹)	(2-19 hourly)	were considered as representative hourly averages.

- 1 *From the National Climate Database for New Zealand (NIWA, 2015), all the other parameters
- 2 were measured at the site.
- 3

1 Table 4. Statistics calculated for the comparison of the modelled and measured variables: root
 2 mean square error (RMSE), Pearson's correlation coefficient (r), the equation of the fitted least-
 3 squares equation (x - observation, y - model) and the level of significance of the correlation.

Variable*	RMSE	Equation	r	Level of significance
Ammonia emission flux	43.06 $\mu\text{g N m}^{-2}\text{g}^{-1}$	$y=34.63+0.50x$	0.54	0.01
Soil pH	0.56	$y=3.04+0.64x$	0.75	0.001
Model TAN budget vs. measured soil $\text{NH}_x\text{-N}$	-	-	0.63	0.01
Volumetric water content	0.05 $\text{m}^3 \text{m}^{-3}$	$y=0.10+0.67x$	0.92	0.001

4
 5 * All the modelled and measured variables are the same as shown in Fig. 4. In the case of the
 6 emission flux, we compared the measured flux in the given measurement period with the value
 7 simulated at the time of the midpoint of the corresponding measurement period as explained in
 8 Table 2.

1 Table 5. The percentage of the change in total emitted NH₃ compared to the original run after
 2 modifying the different model constants by -20, -10, +10 and +20%.

Module	Parameters	Total NH ₃ emission change in response to change if parameter by			
		-20%	-10%	+10%	+20%
2LCCPM	z _l (height of the top of logarithmic wind profile)	+0.02%	+0.01%	-0.01%	-0.02%
TAN budget	Δz (thickness of NH ₃ emission layer)	-11.7%	-5.57%	+5.07%	+10.5%
	A _{patch} (area of a urine patch)	+1.39%	+0.67%	-0.58%	-1.61%
Soil pH	β (soil buffering capacity)	+1.29%	+0.64%	-0.62%	-1.22%
	REW (readily evaporable water)	-2.98%	-1.69%	+2.06%	+4.32%
Water budget	θ _{fc} (field capacity)	-18.4%	-6.63%	+6.34	+9.12%
	Θ _{pwp} (permanent wilting point)	+9.48	+4.60%	-4.42%	-8.85%

3

4

1 Table 6. The results of the sensitivity analysis to the different meteorological variables. We
 2 changed these by $\pm \Delta x$ derived based on the minimum and the maximum of the given parameter
 3 over the modelling period ($\Delta x = (\text{Max}-\text{Min})/10$), and calculated the difference in the total
 4 emission over the modelling period compared to the original run. We also calculated the
 5 correlation (r) between the original input variables and the modelled hourly NH_3 emission
 6 fluxes.

Variable	Min	Max	Δx	Total NH_3 emission change in		r
				response to change in parameter by		
				$-\Delta x$	$+\Delta x$	
u (ms^{-1})	0.62	8.59	0.80	-5.5%	+4.7%	0.40
T_{soil} ($^{\circ}\text{C}$)	11.6	27.9	1.64	-2.6%	+2.7%	0.58
p (kPa)	99.9	102.3	0.24	+0.0%	-0.0%	-0.33
T_{air} ($^{\circ}\text{C}$)	13.5	29.0	1.56	-2.4%	2.9%	0.60
R_{glob} ($\text{MJ m}^2 \text{ h}^{-1}$) ^a	0.00	3.32	0.33	-2.0%	+4.1%	0.32
RH (%) ^b	30	95	6.50	+9.1%	-8.6%	-0.49
RH (%) ^b	only for evaporation ^c			+3.2%	-2.8%	-
P (mm) ^d	0.00	0.83	0.08	-0.7%	+0.8%	-
T_{air} and T_{soil} ($^{\circ}\text{C}$)	-	-	-	-4.9%	+5.7%	-

7 ^aWhen changed by $-\Delta x$, negative values were replaced by 0.

8 ^bWhen changed by $+\Delta x$, values greater than 100% were reduced to 100%.

9 ^cIn this test RH was modified by the same extent but only in the evaporation module.

10 ^dThe hourly precipitation sum was changed only in the hours when there was precipitation
 11 originally.

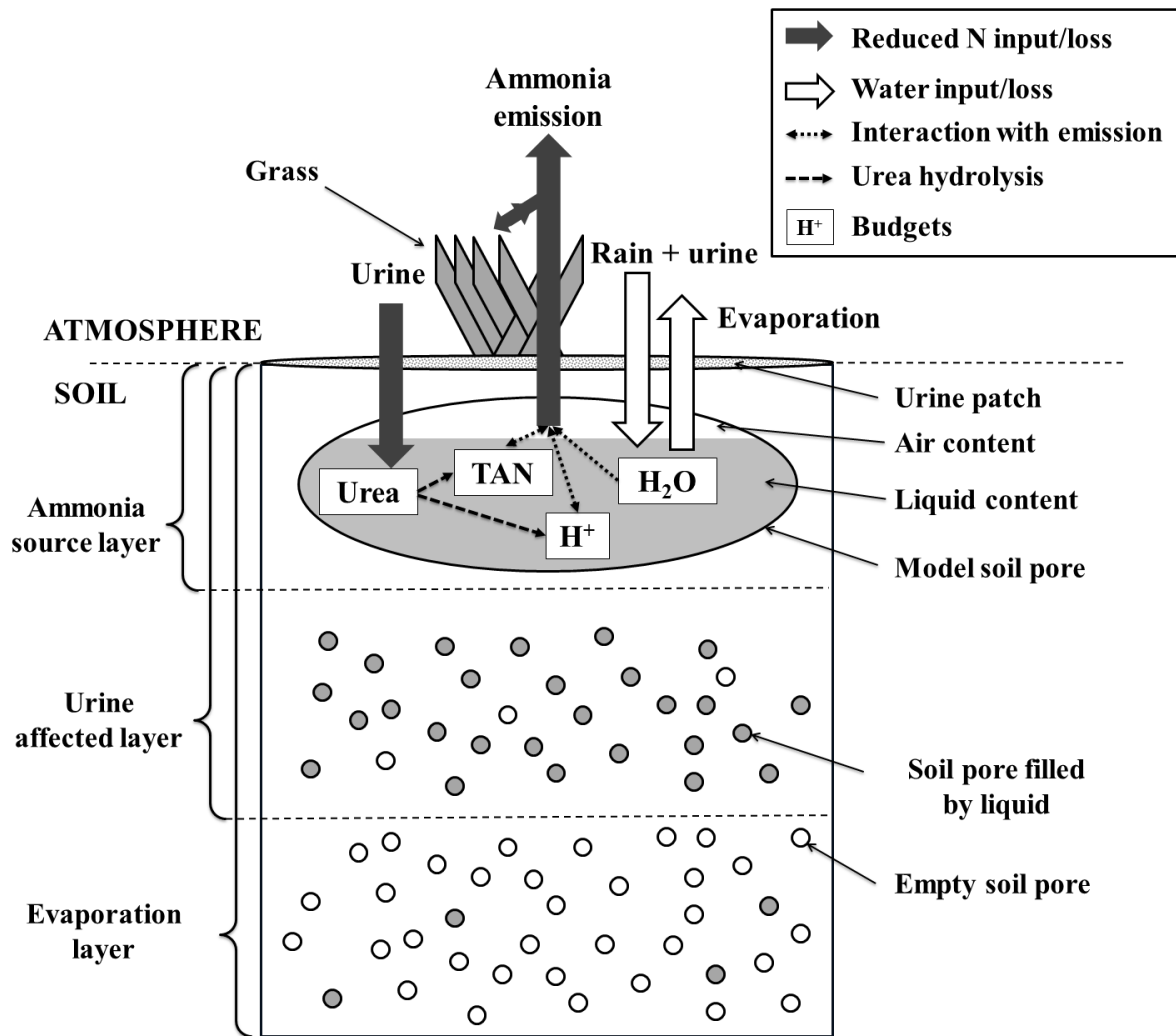
12

1 Table 7: Comparison of the total emission (g N) from a single urine patch from the model runs
2 assuming different N content of the urine deposited with the original temperature and +10°C
3 (both in air and the soil temperature) scenario. We also calculated Q10 as the ratio of the total
4 emission for the original and the amended temperature scenario.

	Total emission (g N)		
	Original	+10 °C	Q ₁₀
Base run	95.8	121.0	1.26
3x N content	290.4	370.8	1.28
5x N content	489.7	613.8	1.25

5

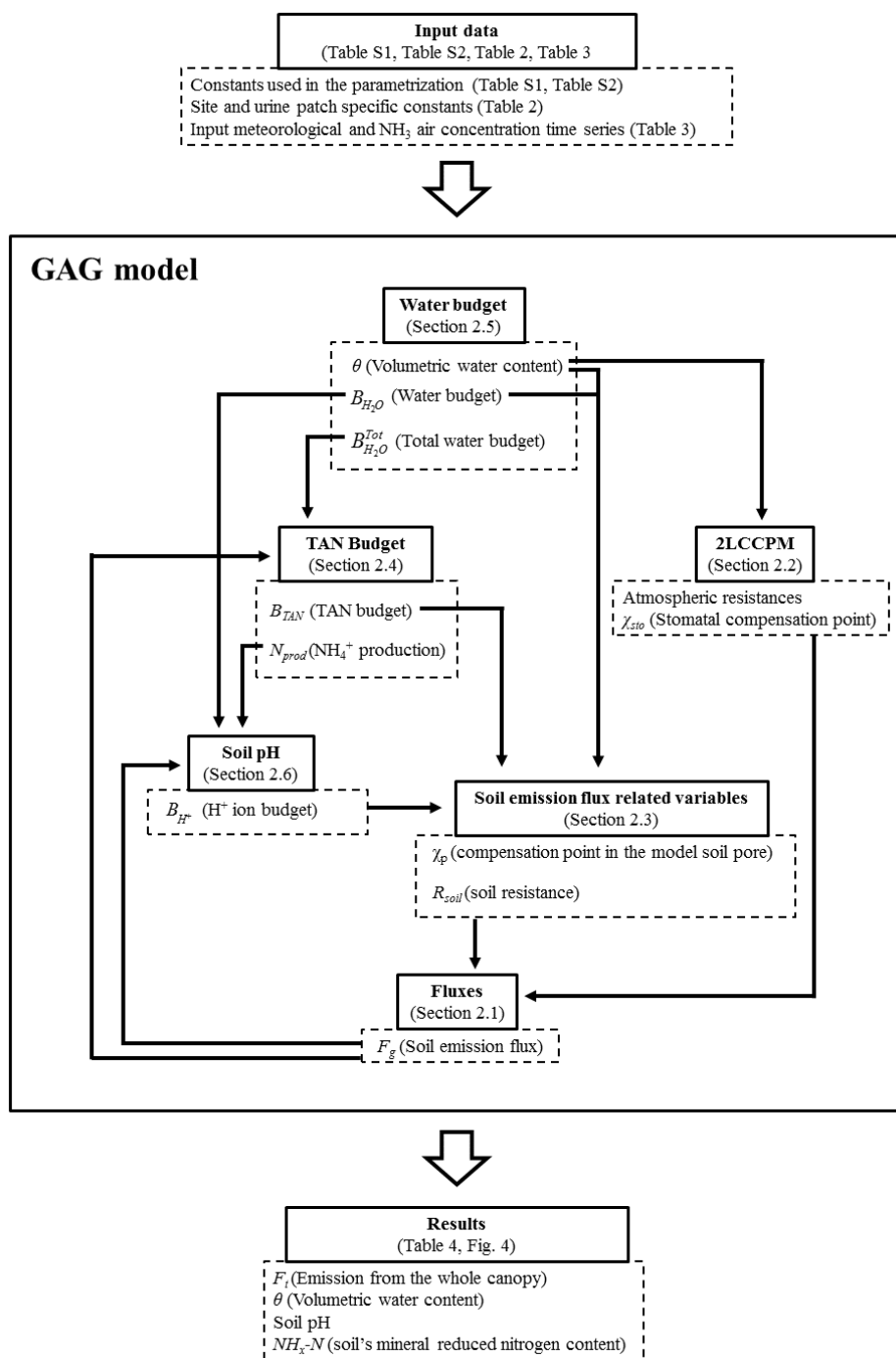
6



1

2

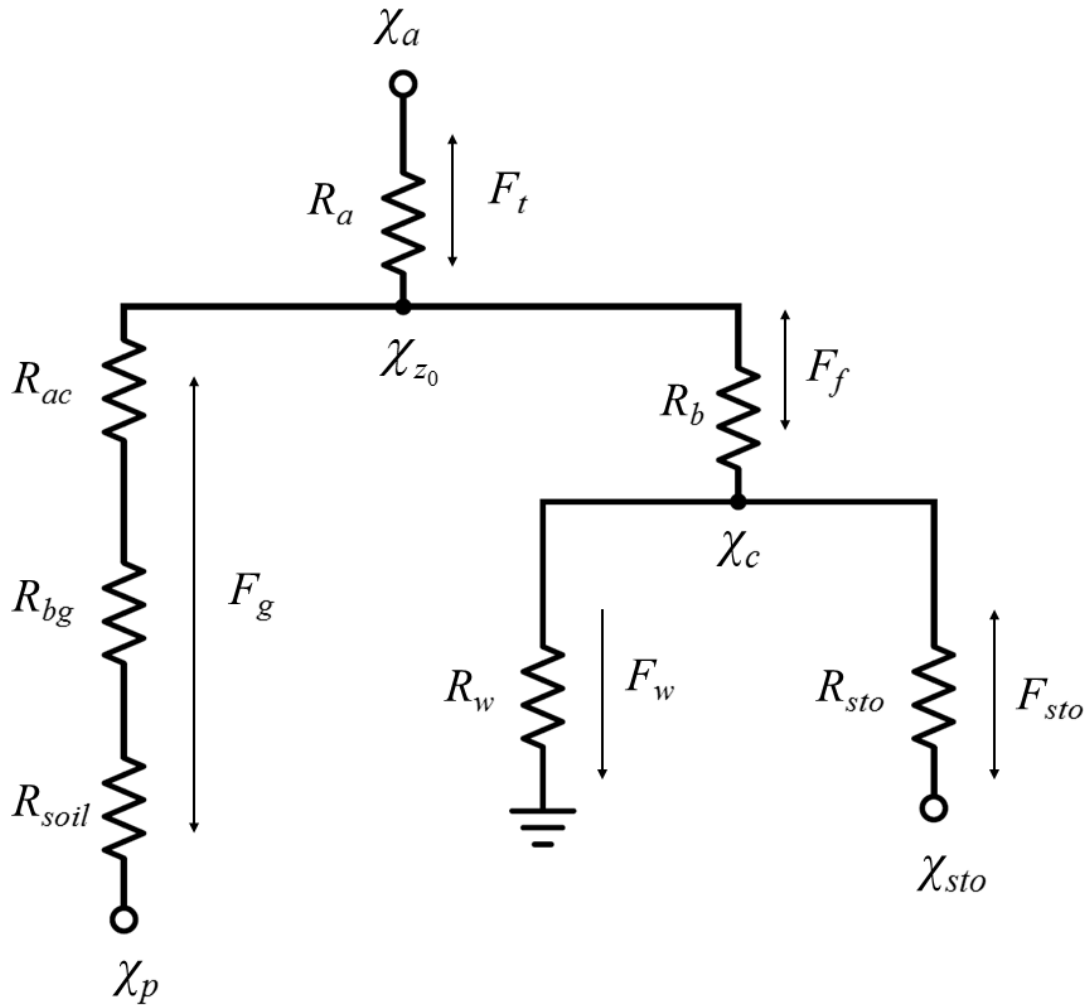
3 Figure 1. Schematic of major relationships in the GAG model. Empty soil pores in the middle
 4 layer represents that the maximum water content in the model is field capacity instead of being
 5 saturated. Whilst in the bottom layer the soil pores filled by liquid represents that the lowest
 6 water content is at the permanent wilting point instead of being completely dry. For more details
 7 on schematic see the text of Section 2.



1

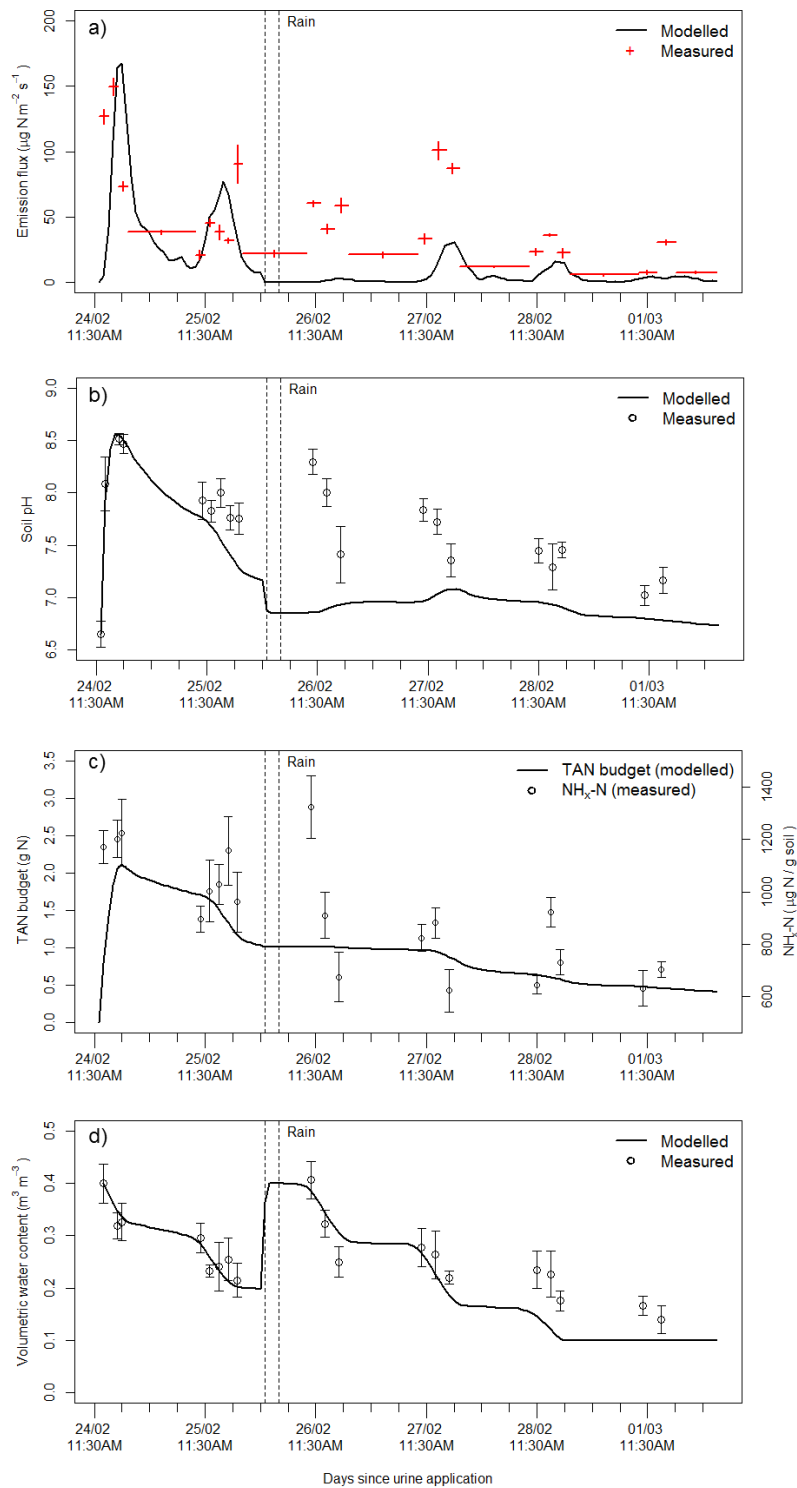
2

3 Figure 2. A flowchart depicting the steps of the calculation in the GAG model (middle panel),
 4 processing the input data (top panel) to the results that were compared with measurements in
 5 this study (bottom panel). The figure indicates the key variables that are carried from one
 6 module to another module(s). The figure, table and section numbers referred in the figure show
 7 where further description of the different model parts can be found in this paper. (2LCCPM
 8 stands for Two-Layer Canopy Compensation Point Model.)



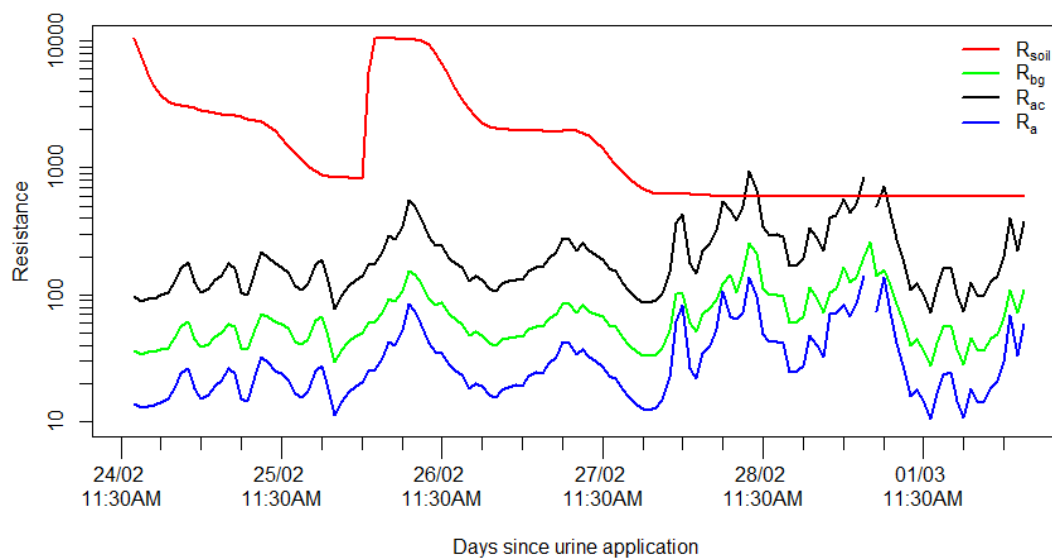
1
2
3
4
5
6
7
8

Figure 3. The network of gaseous resistances (R), ammonia concentrations (χ) and ammonia fluxes (F) used in the GAG model, which is based on the two-layer canopy compensation point model of Nemitz et al. (2001) incorporating concentration of the soil pore (χ_p) and soil resistance (R_{soil}). For the description of the other parameters in the framework see the text of this section.



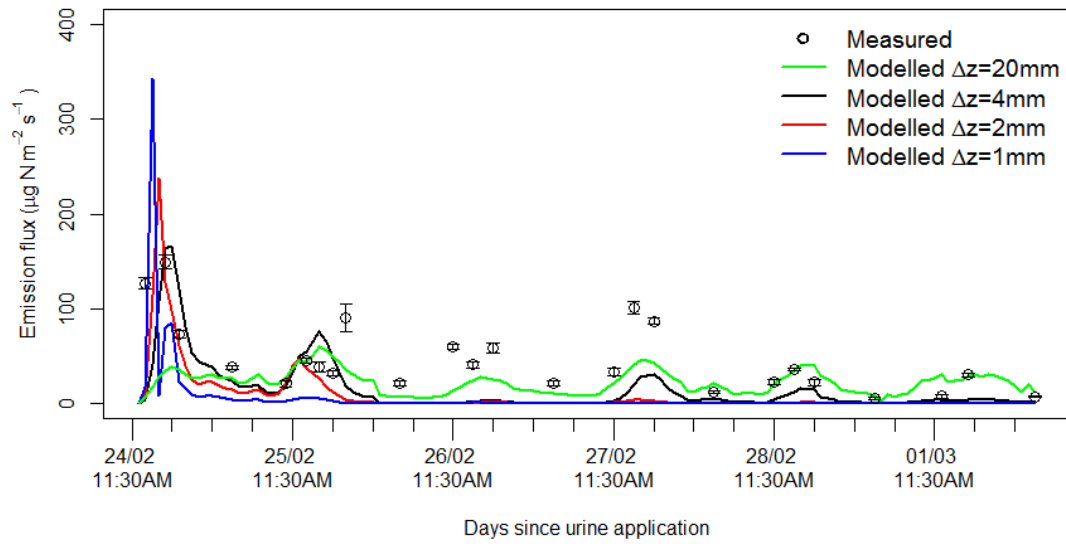
1
2
3
4
5
6
7

Figure 4. Comparison of modelled and measured values for NH_3 emission flux with the corresponding sampling periods of the measurements (a), soil pH (b), TAN budget and $\text{NH}_x\text{-N}$ (c), and volumetric water content of the top 5 mm layer of the soil (d). The vertical error bars stand for the standard deviation in the measurements.



1
2
3
4
5
6

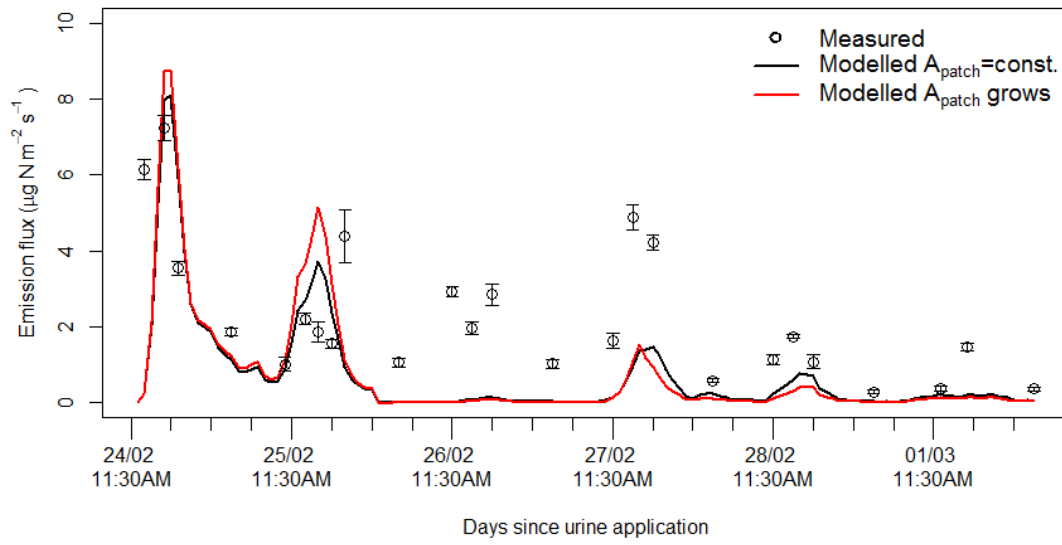
Figure 5. The atmospheric and the soil resistances over the modelling period. (At the time of the missing values in R_{bg} , R_{ac} and R_a u^* was 0, for which resistances are infinite. In these cases emission flux was assumed to be 0.)



- 1
- 2
- 3
- 4

Figure 6. NH₃ fluxes from a urine patch with different Δz values.

1

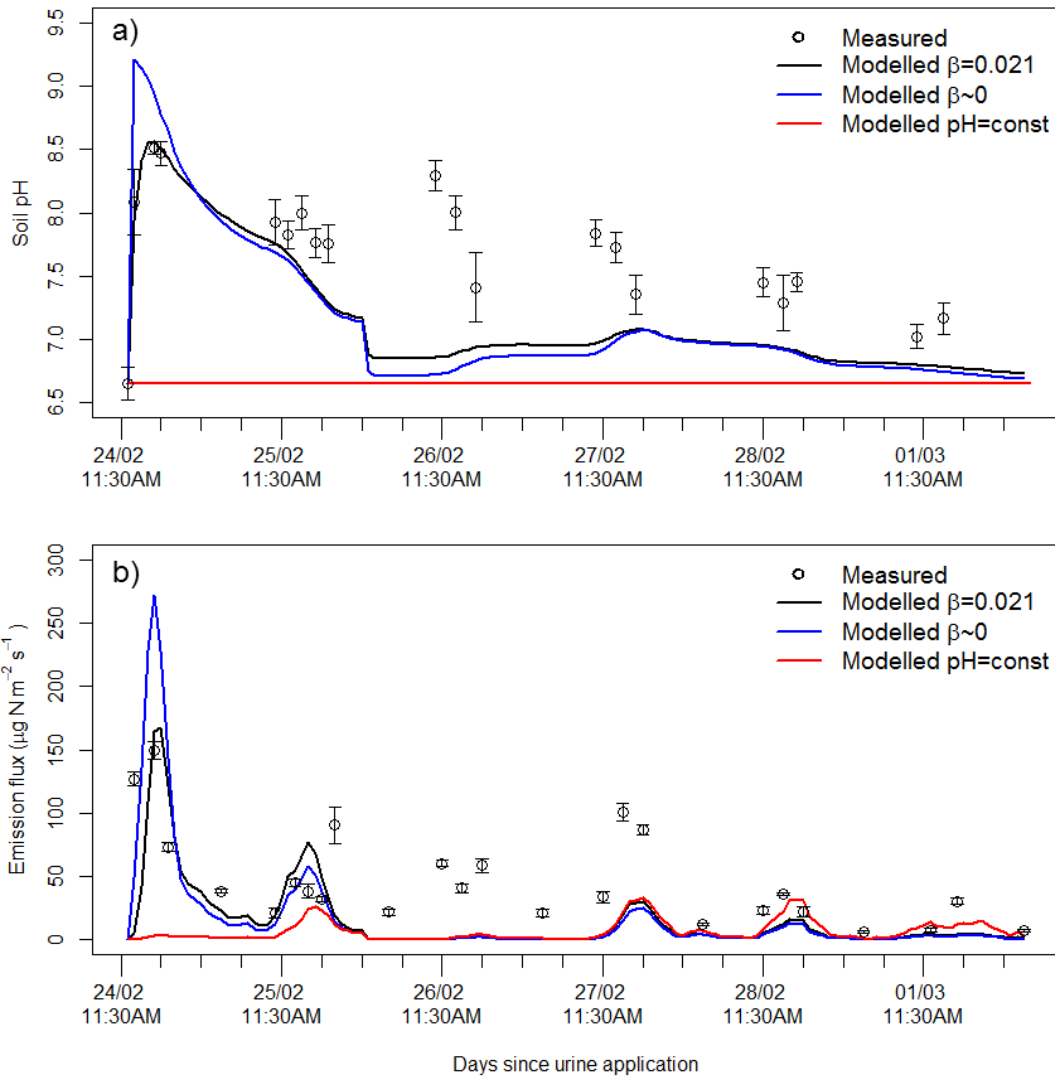


2

3

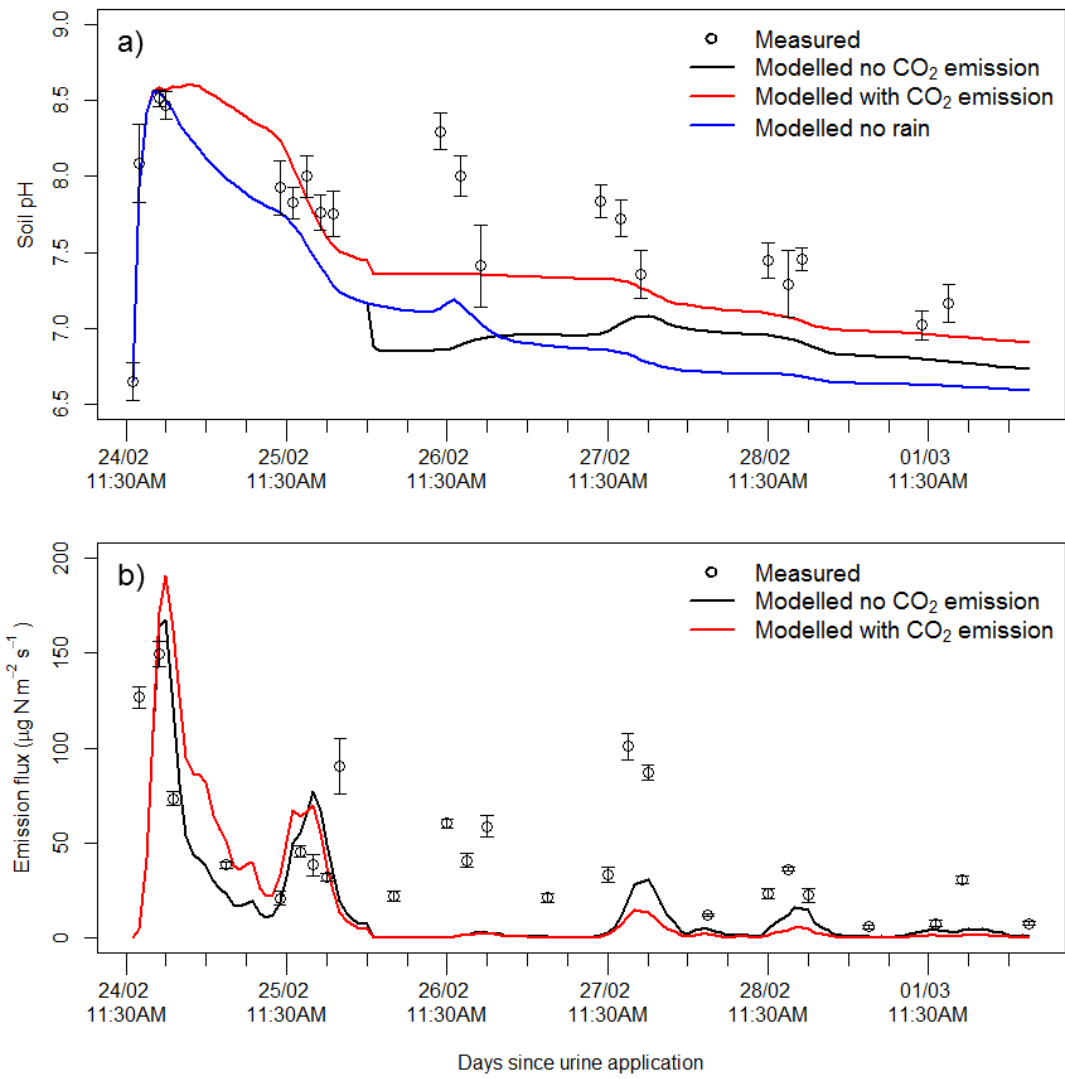
4 Figure 7. NH_3 fluxes from the whole experimental area with constant and with gradually
5 growing urine patches.

6



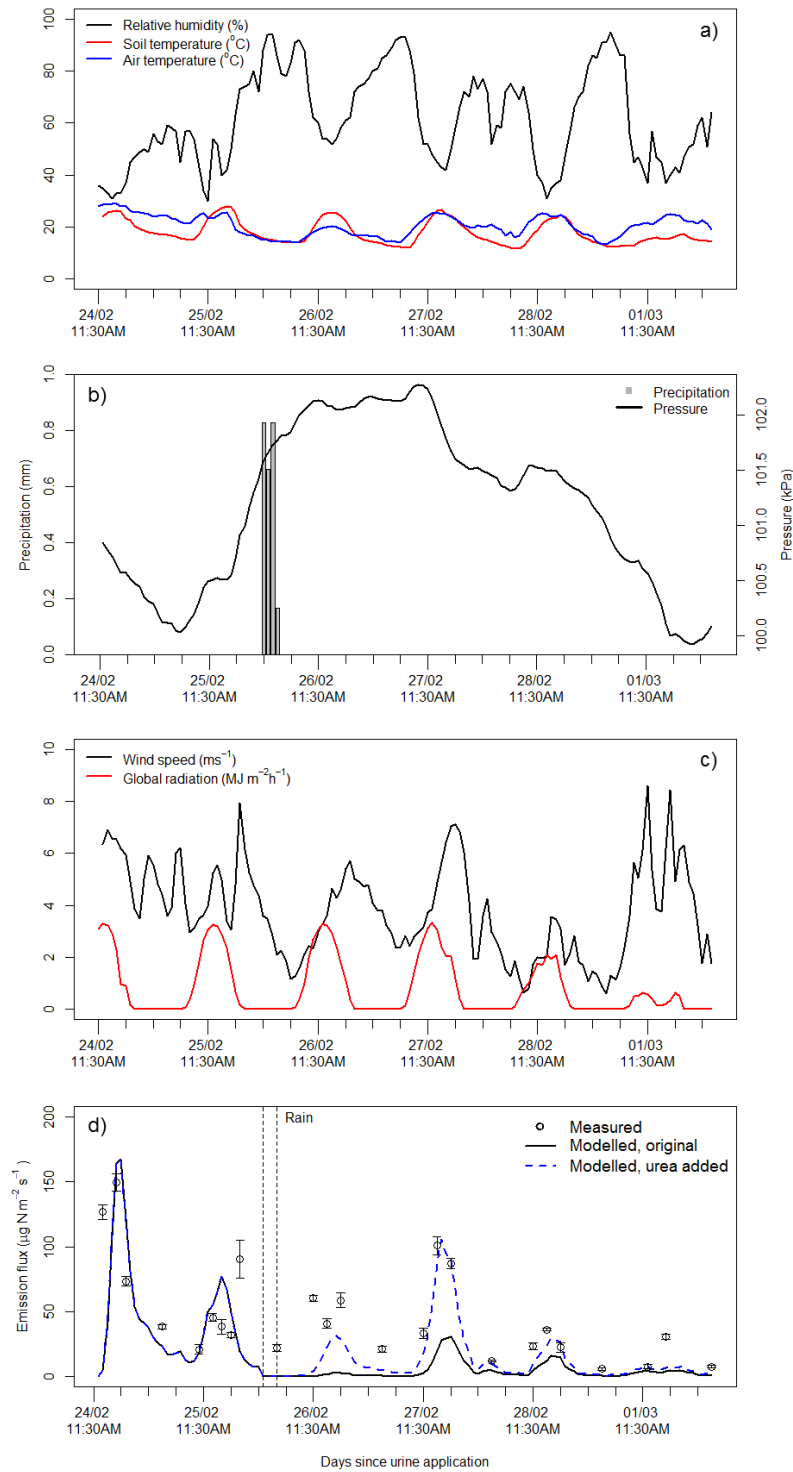
1
2
3
4
5
6

Figure 8. Soil pH under a urine patch (a) and NH₃ emission from it (b) with the currently applied buffering capacity ($\beta = 0.021$, original run), with no buffering ($\beta = 0$) and with constant pH, together with the measured values.



1
2
3
4
5
6

Figure 9. Soil pH under a urine patch (a) and NH₃ emission from it (b) without CO₂ emission (original run) and with an assumed CO₂ emission. On panel a) the original run without rain is also plotted.

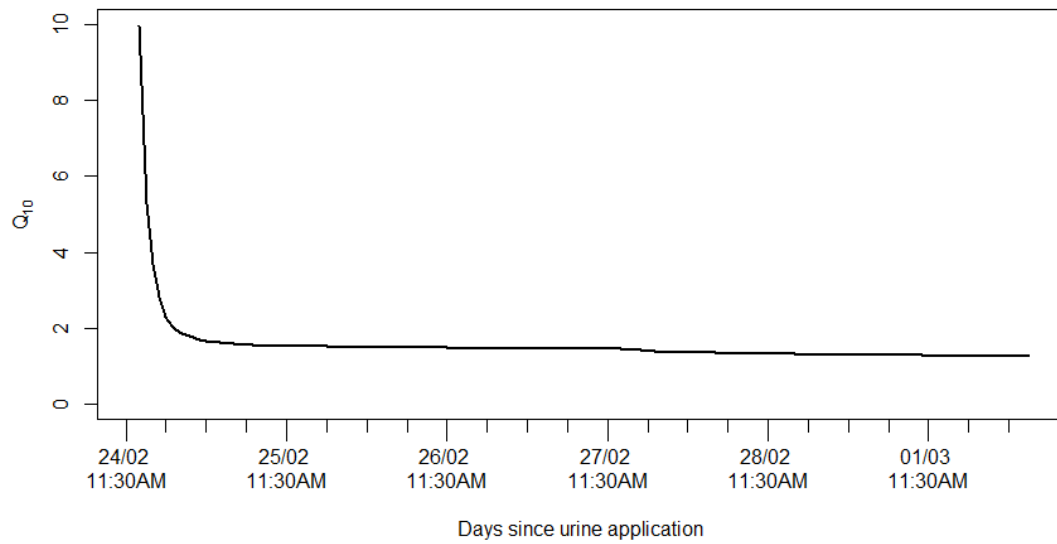


1

2

3 Figure 10. The investigated meteorological variables (relative humidity, soil and air
 4 temperature (a), precipitation and surface pressure (b), wind speed and global radiation (c)) and
 5 the hourly NH₃ fluxes (d) simulated by the original model (black line) and the modified model

- 1 (dashed blue line), in which fresh urea was assumed to washed into the soil during the rain
- 2 event.
- 3



- 1
- 2 Figure 11. Calculated Q_{10} values for the cumulative NH_3 emissions between urine application
- 3 and the given time step.